CHEMISTRY
A EUROPEAN JOURNAL

DOI: 10.1002/chem.200902406

Intermediates Involved in the Oxidation of Nitrogen Monoxide: Photochemistry of the *cis*-$N_2O_2{\cdot}O_2$ complex and of *sym*-N_2O_4 in Solid Ne Matrices

Helmut Beckers,* Xiaoqing Zeng, and Helge Willner[a]

Abstract: Pure *sym*-N_2O_4 isolated in solid Ne was obtained by passing cold neon gas over solid N_2O_4 at −115 °C and quenching the resulting gaseous mixture at 6.3 K. Filtered UV irradiation (260–400 nm) converts *sym*-N_2O_4 into *trans*-$ONONO_2$, a weakly interacting $(NO_2)_2$ radical pair, and traces of the *cis*-$N_2O_2{\cdot}O_2$ complex. Besides the weakly bound $ON{\cdot}O_2$ complex, *cis*-$N_2O_2{\cdot}O_2$ was also obtained by co-deposition of NO and O_2 in solid Ne at 6.3 K, and both complexes were characterised by their matrix IR spectra. Concomitantly formed *cis*-N_2O_2 dissociated on exposure to filtered IR irradiation (400–8000 cm^{-1}), and the *cis*-$N_2O_2{\cdot}O_2$ complex rearranged to *sym*-N_2O_4 and *trans*-$ONONO_2$. Experiments using $^{18}O_2$ in place of $^{16}O_2$ revealed a non-concerted conversion of *cis*-$N_2O_2{\cdot}O_2$ into these species, and gave access to four selectively di-^{18}O-substituted *trans*-$ONONO_2$ isotopomers. No isotopic scrambling occurred. The IR spectra of *sym*-N_2O_4 and of *trans*-$ONONO_2$ in solid Ne were recorded. IR fundamentals of *trans*-$ONONO_2$ were assigned based on experimental $^{16/18}O$ isotopic shifts and guided by DFT calculations. Previously reported contradictory measurements on *cis*- and *trans*-$ONONO_2$ are discussed. Dinitroso peroxide, ONOONO, a proposed intermediate in the IR photoinduced rearrangement of *cis*-$N_2O_2{\cdot}O_2$ to the various N_2O_4 species, was not detected. Its absence in the photolysis products indicates a low barrier ($\leq$10 kJ mol^{-1}) for its exothermic O–O bond homolysis into a $(NO_2)_2$ radical pair.

Keywords: matrix isolation · nitrogen oxides · radicals · reactive intermediates · vibrational spectroscopy

Introduction

Recently we have investigated a weakly bound doublet $ON{\cdot}O_2$ complex formed by co-deposition of NO and molecular oxygen in a Ne matrix at 6.3 K, as well as its reversible photochemical interconversion into the NO_3 free radical upon exposure of the matrix to near-UV and visible light.[1] During these experiments we noticed the formation of various N_2O_4 species by either thermal or photochemical reactions. Because such binary nitrogen oxides are of considerable significance in tropospheric air pollution,[2] physiological systems,[3,4] and industrial processes,[5] we decided to explore in more detail the formation of these N_2O_4 species by photochemical isomerisation of *sym*-N_2O_4 (D_{2h}) and from NO and molecular O_2 isolated in solid Ne.

A huge number of reports have already appeared on N_2O_4 species, and we are not inclined to give a comprehensive overview. N_2O_4 derivatives were investigated in the liquid[6–8] and solid state;[9–12] in liquid rare gases;[13,14] organic solvents;[6,15,16] in various solid matrices such as Ne,[17] Ar,[18–21] N_2[22] and O_2;[19,20] and adsorbed on amorphous and crystalline water–ice films.[23,24] These studies have shown that two NO_2 radicals in principle may combine to various N_2O_4 species. Only *sym*-N_2O_4, in which the two NO_2 moieties are linked with a N–N bond, was the subject of gas-phase[25–28] and high-level ab initio investigations.[29–32] As the most stable isomer, it is expected to be formed preferential-

[a] Dr. H. Beckers, Dr. X. Zeng, Prof. Dr. H. Willner
Fachbereich C—Anorganische Chemie
Bergische Universität Wuppertal
42097 Wuppertal (Germany)
Fax: (+49) 202-439-3053
E-mail: beckers@uni-wuppertal.de

Supporting information for this article is available on the WWW under http://dx.doi.org/10.1002/chem.200902406. It contains a complete list of absorptions observed between 200–3000 cm^{-1} after exposure of Ne/$^{16}O_2$/NO and Ne/$^{18}O_2$/NO samples at 6.3 K to filtered IR radiation (Table S1); a comparison of observed fundamentals of various molecular $ONONO_2$ species with calculated harmonic frequencies of *cis*-like $ONONO_2$ (Table S2); as well as optimised geometries and harmonic vibrational frequencies of *trans*- and *cis*-like $ONONO_2$ species (see Figure S1) calculated using ab initio SCS-MP2 (Tables S5 and S10), DFT (Tables S3, S4 and S9), and DFT-D methods (Tables S5–S8 and S11).

ly when NO_2 diluted in inert gases is deposited at cryogenic temperatures. However, such experiments revealed substantial formation of the less stable nitroso nitrate, $ONONO_2$.[18–20,22] The preferred asymmetric dimerisation of NO_2 to $ONONO_2$ in solid matrices rather than to *sym*-N_2O_4 was explained by dipole–dipole attraction of the reacting NO_2 pair favouring the O–N approach.[18]

The reaction between NO and molecular oxygen has been extensively studied in the past in gaseous[33] and condensed phases,[21] and in aqueous solutions as well.[34] The thermal reaction of NO with molecular O_2, studied in solid oxygen and argon matrices at about 30 K, yield nitroso nitrate, $ONONO_2$,[35,36] whereas in the gas phase this well-known reaction produces NO_2 [Eq. (1)]:[33]

$$2\,NO + O_2 \rightarrow 2\,NO_2 \qquad \Delta H^{\ominus} = -114\ kJ\,mol^{-1} \tag{1}$$

This reaction [Eq. (1)] provided the earliest known, and perhaps the most frequently cited example of a trimolecular reaction,[33] but its mechanism is still under discussion.[37,38] This controversy initiated some recent computational studies on its mechanism and of the N_2O_4 potential-energy surface (PES).[39–41] The most detailed of these studies appeared very recently.[41]

As one would expect from the known chemistry of nitrogen oxides,[42] these studies revealed a rather complex system and a remarkable large number of molecular N_2O_4 species, which are found to be thermodynamically stable with respect to decomposition. Table 1 lists those species that may be envisioned and includes the ionic nitrosonium nitrate, $NO^+NO_3^-$.[15,24,43–47] Those species that are proposed to be involved in the oxidation of NO by O_2 are marked by a tick. Although many of these species may exist only as short-lived intermediates in the gas phase, if they are prevented from reacting to form more stable species, as for example, by isolation in rare-gas matrices, they can in principle be detected and characterised by using spectroscopic techniques.

Table 1. Various N_2O_4 isomers and their proposed involvement in the $NO + O_2$ reaction.[a]

Experimentally known	Unknown species
sym-N_2O_4 (O_2N–NO_2) (✓)	$N_2O_2{\cdot}O_2$ complex (✓)
ON–ONO_2 (✓)[c]	$(NO_2)_2$ radical pairs (✓)
$NO^+NO_3^-$	ON-OO-NO (✓)[b]

[a] Species proposed to be involved in the oxidation of NO by O_2 are marked by a tick. [b] Three different isomers of dinitroso peroxide may exist with respect to the corresponding nitrosooxy ON–O single bonds: *s-cis,cis*, *s-cis,trans* and *s-trans,trans.* [c] Two isomeric forms of nitroso nitrate may exist with respect to the corresponding nitrosooxy ON–O single bonds: *s-cis*-and *s-trans.*

It is currently generally accepted that dinitroso peroxide, ON-OO-NO, will be formed in an early stage of Equation (1).[39–41] However, it is not yet settled whether its formation is the initial stage in the oxidation process, as has been reinforced by a recent computational study,[41] or the peroxide is formed via a primary intermediate. On the other hand, it is now well established, that NO and O_2 form molecular complexes,[48,49] and since NO ($X\ ^2\Pi$) and O_2 ($X\ ^3\Sigma_g^-$) have one and two unpaired electrons, respectively, both quartet- and doublet-state molecular complexes may be considered.[50] In the case of the doublet-state $ON{\cdot}O_2$ complex in particular, which benefits from spin pairing,[39,48] is difficult to describe it correctly by theory.[51,52] However, convincing evidence for its existence comes from various experimental studies, such as recent matrix-isolation work, in which this complex was characterised by its IR and UV spectra,[1,53] as well as from neutralisation reionisation mass spectrometry,[54] electron paramagnetic resonance (EPR) spectroscopy in frozen organic solutions[55] and in the gas phase[38] and cyclic voltammetry on $ONOO^-$ in aqueous solution.[56] These studies also provide structural implications[54,55] and lifetimes for this complex under various conditions.[54–56] It, thus, seems reasonable that the two-step [Eqs. (2) and (3)] formation of the peroxide via the $ON{\cdot}O_2$ intermediate will be favoured with a large excess of O_2 under atmospheric conditions rather than the concerted trimolecular reaction pathway.[57]

$$NO + O_2 \rightleftharpoons ON \cdot O_2 \qquad \Delta H^{\ominus} \approx -2\ kJ\,mol^{-1} \tag{2}$$

$$ON \cdot O_2 + NO \rightarrow ON\text{-}OO\text{-}NO \qquad \Delta H^{\ominus} \approx -39\ kJ\,mol^{-1} \tag{3}$$

Dinitroso peroxide has never been detected experimentally.[58] Due to its negative O–O bond-dissociation energy and the unusually low barrier for its O–O bond dissociation,[39,40] it is predicted to decompose rapidly to form a weakly bound $(NO_2)_2$ radical pair [Eq. (4)].[39–41]

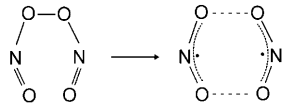

s-cis,cis-dinitroso peroxide $(NO_2)_2$ (C_{2h})

$$\Delta H^{\theta} \approx -74\ kJ\,mol^{-1} \tag{4}$$

Although such $(NO_2)_2$ dimers may rapidly dissociate in the gas phase to form $2\,NO_2$ free radicals, they might be trapped as a radical pair in low-temperature rare-gas matrices, because significant activation barriers have been predicted theoretically for their rearrangement into $ONONO_2$ and *sym*-N_2O_4.[40,41] Weakly bound $(NO_2)_2$ radical pairs probably play a crucial role also in the *sym*-N_2O_4–*trans*-$ONONO_2$ isomerisation, for which computational attempts to find a low-energy pathway failed,[41,59–61] or in the rapid gas-phase isotopic exchange reactions of isotopically labelled NO_2 [Eq. (5)]:[62]

$$NO_2 + N^{18}O_2 \rightleftharpoons 2\,N(^{16}O)^{18}O \tag{5}$$

Despite the large body of experimental and computational studies devoted to weakly bound N_2O_4 species, our knowl-

edge particularly about nitroso nitrate remained scarce. Nitroso nitrate, $ONONO_2$, was proposed to play an important part in the condensed state chemistry of NO_2, such as the self-ionisation of dinitrogen tetraoxide leading to nitrosonium nitrate $NO^+NO_3^-$,[15,24,43,44,46,47] and its hydrolysis to nitrous (HONO) and nitric acid ($HONO_2$).[24,63] But only limited work has been reported on the thermochemistry of this less stable N_2O_4 isomer,[7] and even the dissociation enthalpy of *trans*-$ONONO_2$ into $2NO_2$ has, to our knowledge, not been measured experimentally. It may be estimated to be about 38 kJ mol^{-1} from the experimental enthalpies of the *sym*-N_2O_4–*trans*-$ONONO_2$ isomerisation ($\Delta H^\ominus$= 19 kJ mol^{-1})[7] and the dissociation of *sym*-N_2O_4 into $2NO_2$ (57 kJ mol^{-1}) [Eqs. (6)–(8)]:[25]

$$sym\text{-}N_2O_4 \rightleftharpoons 2NO_2 \qquad \Delta H^\ominus = 57\ \mathrm{kJ\,mol^{-1}} \tag{6}$$

$$trans\text{-}ONONO_2 \rightleftharpoons sym\text{-}N_2O_4 \qquad \Delta H^\ominus \approx -19\ \mathrm{kJ\,mol^{-1}} \tag{7}$$

$$trans\text{-}ONONO_2 \rightleftharpoons 2NO_2 \qquad \Delta H^\ominus \approx 38\ \mathrm{kJ\,mol^{-1}} \tag{8}$$

On the other side, the mechanisms of both the *sym*-N_2O_4–*trans*-$ONONO_2$ isomerisation and the asymmetric NO_2 dimerisation, $2NO_2 \rightarrow$*trans*-$ONONO_2$, are still unknown. Furthermore, predicted barriers for the asymmetric NO_2 dimerisation varied substantially.[40,41,64] In contrast, the symmetric dimerisation to *sym*-N_2O_4 was found experimentally and computationally to proceed barrier-free.[29]

Former matrix-isolation studies related to this work were seriously hampered by the complex mixtures that were obtained by co-deposition of NO and O_2 in solid O_2[21] and Ar,[36] and annealing of these deposits to about 30 K.[36,42] Under these conditions, diffusion of NO and O_2 within the solid matrices cannot be prevented and, in addition to various N_2O_4 derivatives, different N_2O_3 isomers were formed from the reaction $NO+NO_2$. Furthermore, the observed N_2O_4 species might be formed either by means of the initial reaction sequence shown in Equations (2)–(4), or, alternatively, from the reaction between a NO dimer and O_2. The most stable NO dimer, easily formed in solid matrices, is the weakly bound *cis*-ONNO (*cis*-N_2O_2).[65]

The purpose of our Ne matrix-isolation study is to get more insight into the mechanism of the nitric oxide oxidation in inert matrices, and to search for the hitherto unknown weakly bound N_2O_4 species listed in Table 1. We describe the UV photolysis of pure *sym*-N_2O_4, the selective IR photolysis of a hitherto unknown *cis*-$N_2O_2{\cdot}O_2$ complex isolated in solid neon at 6.3 K, and the vibrational spectrum of *trans*-$ONONO_2$, as well as $^{16/18}O$ isotopic-labelling experiments.

Results and Discussion

UV photolysis of *sym*-N_2O_4 in solid Ne: Passing Ne over solid *sym*-N_2O_4 at −115 °C and subsequent quenching of the resulting gaseous mixture at 6.3 K yielded a Ne matrix containing *sym*-N_2O_4 with a small amount of NO_2. The corresponding IR spectrum of this matrix is depicted in Figure 1, upper trace. Apart from the NO_2 monomer band located at 1613.5 cm^{-1} (marked by an asterisk) all other bands are at-

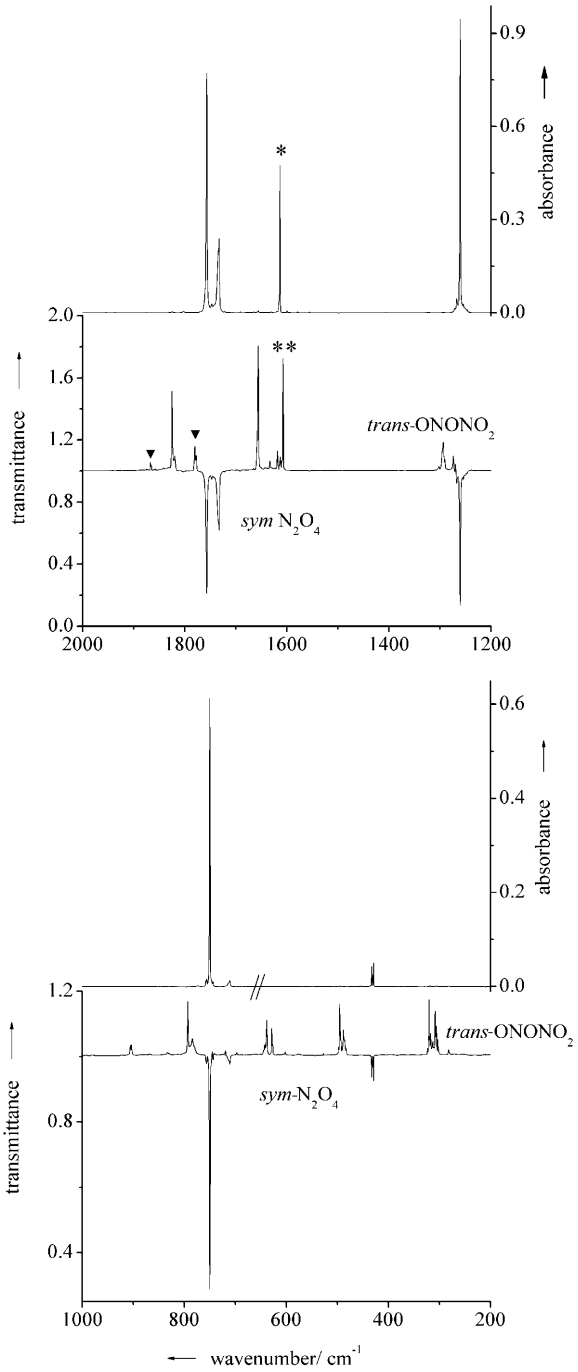

Figure 1. IR spectra obtained from *sym*-N_2O_4 highly diluted in Ne at 6.3 K in the wavenumber range 200–1000 (lower panel) and 1200–2000 cm^{-1} (upper panel). In each of the panels the initial deposit is shown in the upper trace, and the difference spectrum obtained from spectra after−before irradiation with filtered UV light (λ = 260-400 nm) are depicted in the lower traces. Absorptions due to the NO_2 monomer, a weakly bound $(NO_2)_2$ dimer, and the *cis*-$N_2O_2{\cdot}O_2$ complex are marked by one asterisk, two asterisks and an arrowhead, respectively.

tributed to *sym*-N_2O_4 by comparison with reported frequencies.[66] This assignment is supported by the simultaneous decrease of these bands when the deposit was subjected to filtered UV light in the $\lambda = 260$–400 nm range. The behaviour of N_2O_4 bands upon photolysis is shown in the difference spectrum displayed as the lower traces in Figure 1.

The strong ν_3 IR mode of NO_2 is the only fundamental observed in the solid matrix.[67] Four of the five infrared-active fundamentals of *sym*-N_2O_4 (D_{2h}) are shown in Figure 1 at 1756.8 (vs, ν_9, b_{2u}), 1260.5 (vs, ν_{11}, b_{3u}), 749.7 (vs, ν_{12}, b_{3u}) and 429.1 cm^{-1} (w, ν_7, doublet, b_{1u}).[66,68] A band at 1732.7 cm^{-1} (m) and a much weaker absorption at 710.6 cm^{-1} (vw) are combination bands of *sym*-N_2O_4.[66] These bands correspond to absorptions previously observed at 1733 cm^{-1} (gas phase) and at 708 cm^{-1} (liquefied xenon), respectively.[66] The weak out-of-plane deformation ν_7 (b_{1u}) has not been reported for a matrix before. This band appeared as a doublet (432.5 and 429.1 cm^{-1}), probably due to matrix site splitting, and is close to the gas-phase value (425 cm^{-1}).[69] The rocking NO_2 fundamental (ν_{10}, b_{2u}), attributed to a weak band at 265 cm^{-1} in solid N_2O_4,[66] was not detected in our matrix spectra.

The new absorptions that appeared after UV ($\lambda = 260$–400 nm) photolysis were attributed to three different N_2O_4 species: *trans*-$ONONO_2$, the *cis*-$N_2O_2{\cdot}O_2$ complex (marked with an arrowhead), and a weakly bound $(NO_2)_2$ dimer (marked by two asterisks). The NO stretching absorptions of the *cis*-$N_2O_2{\cdot}O_2$ complex produced by photolysis exhibit only small shifts (≤ 1.2 cm^{-1}) from those of *cis*-N_2O_2 deposited from the gas phase. Furthermore, the difference IR spectrum revealed that the intensity of the NO_2 monomer band remains almost unchanged during the photolysis, but a strong new band appeared upon irradiation, which is slightly shifted from the NO_2 monomer band by -6.1 cm^{-1} and marked by two asterisks. The new single band is tentatively attributed to a $(NO_2)_2$ radical pair trapped in the nearest-neighbour position. The expected recombination of this radical pair to a stronger bound N_2O_4 species probably fails due to geometric constraints in the low-temperature matrix.

As shown in Table 2, the observed band positions of the third photolysis product agree quite well with those calculated at the DFT B3LYP/311+G(2d) level of theory for *trans*-$ONONO_2$. Nine fundamentals of *trans*-$ONONO_2$ are shown in the lower traces of Figure 1, and have been unambiguously assigned in Table 2. An approximate description of the corresponding vibrational modes is also listed in Table 2. Three additional very weak fundamentals are predicted below 210 cm^{-1}. A more detailed discussion of the vibrational spectrum of *trans*-$ONONO_2$ will be presented in a separate section below.

Table 2. Observed band positions [cm^{-1}] in solid Ne and calculated fundamental frequencies of *trans*-$ONONO_2$ and their approximate mode description.

		trans-$ONONO_2$		
ν_i	exptl, Ne[a]	calcd[b]		mode
ν_1	1824.9 (s)	1916 (393)	a′:	N=O stretch
ν_2	1656.2 (s)	1685 (411)		NO_2 *a*-stretch
ν_3	1293.2 (m)	1321 (316)		NO_2 *s*-stretch
ν_4	903.3 (w)	940 (38)		N^3–O^4 stretch[c]
ν_5	792.9 (m)	795 (223)		NO_2 bend/N^3–O^4 stretch[c]
ν_6	639.0 (m)	643 (148)		$O^2N^3O^4$ bend[c]
ν_7	488.2 (m)	488 (178)		O^1NO^4/O^4NO^6 bend[c]
ν_8	306.0 (m)	291 (269)		O^4–N^5 stretch[c]
ν_9	–	206 (<0.1)		$N^3O^4N^5$ bend[c]
ν_{10}	784.1 (w)	781 (11)	a″:	O_2N^3–O^4 umbrella[c]
ν_{11}	–	128 (0.2)		N^3O^4–N^5O^6 torsion[c]
ν_{12}	–	4 (0.8)		O_2N^3–O^4N^5 torsion[c]

[a] Experimental band positions [cm^{-1}] at the most intense matrix site; relative intensities in parentheses: s = strong, m = medium, w = weak. [b] Calculated fundamentals [cm^{-1}] at the DFT B3LYP/311+G(2d) level; absolute intensities [km mol^{-1}] in parentheses. For optimised geometric parameters see Figure 2. [c] Superscripted numbers denote the atomic labels shown in Figure 2.

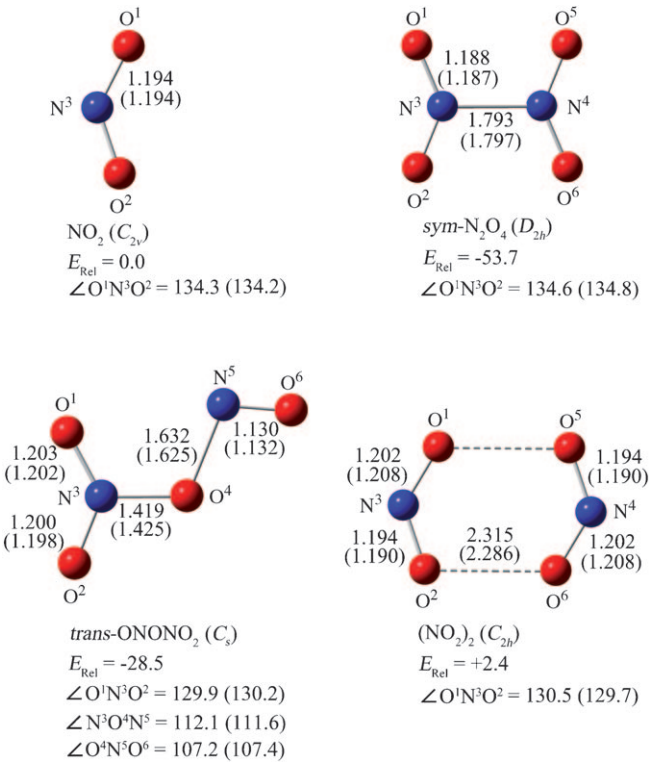

Figure 2. Optimised geometries of NO_2 and various molecular N_2O_4 isomers calculated at the B3LYP/6-311+G(2d) and CBS-QB3 (in parentheses) levels of theory. Calculated bond lengths and angles are denoted in Å and degrees, respectively. Relative energies [kJ mol^{-1}] including ZPE corrections were obtained by using the CBS-QB3 methodology.

Co-deposition of Ne/NO and Ne/O_2/NO mixtures: Figure 3a displays the IR spectrum in the region of the NO stretching vibrations of a Ne/NO (800:1) matrix, deposited at 6.3 K. It reveals a strong NO dimerisation and a variety of distinct sites for both the NO monomer (1877.4, 1874.5 cm^{-1}) and the *cis*-N_2O_2 dimer (ν_1: 1866.7, 1865.5 cm^{-1}; ν_5: 1782.0, 1780.5, 1778.5 cm^{-1}). Both the dimerisation of NO and the photodissociation of $(NO)_2$ dimers have been studied in solid Ne previously.[70,71] In addition to *cis*-N_2O_2, a second dimeric $(NO)_2$ species appears in Ne matrices that give rise to

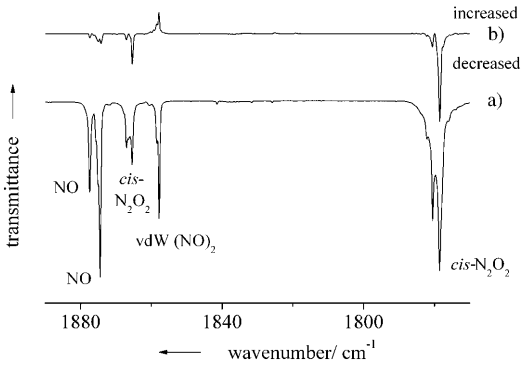

Figure 3. a) IR spectrum of a Ne/NO 800:1 matrix in the region of the NO stretching vibrations, deposited at 6.3 K (apodised resolution 0.25 cm^{-1}; spray-on nozzle cooled to about 85 K). b) Difference spectra obtained from two spectra recorded before and after IR irradiation (400–8000 cm^{-1}).

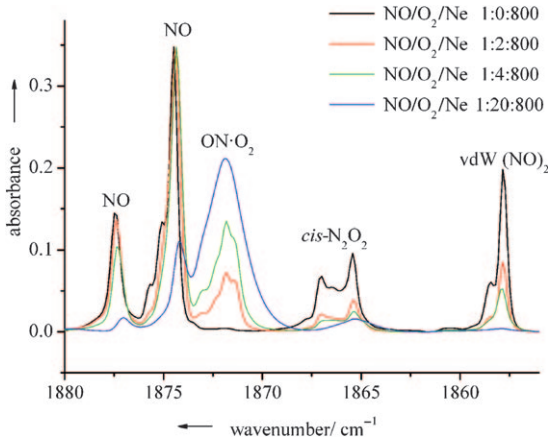

Figure 4. IR spectra of $Ne/O_2/NO$ mixtures with various amounts of O_2 in the region of the NO stretching vibrations and deposited at 6.3 K (spray-on nozzle cooled to about 85 K). Those with $O_2 \leq 0.5\,\%$ are scaled to the most intense NO monomer site.

a rather sharp band at 1857.9 cm^{-1}. According to its concentration dependence, it was attributed to a special van der Waals (vdW) dimer, in which two NO molecules interact more strongly than by the usual dipole–dipole forces in nearest-neighbour positions.[70] Additional bands have been associated with other $(NO)_2$ dimer species in solid Ar and N_2, such as *trans*-N_2O_2[65,71–73] and *cis-/trans*-ONON species.[72,73] However, the band at 1857.9 cm^{-1} and its reversible thermal interconversion with the ν_1 and ν_5 bands of *cis*-N_2O_2 have only been observed in solid Ne.[70]

In an attempt to increase the relative amount of weakly bound *cis*-N_2O_2, the spray-on nozzle was cooled to about 85 K during deposition. Only a small increase of the relative amount of *cis*-N_2O_2 at the expense of both the NO monomer and the vdW $(NO)_2$ dimer was observed. This is in agreement with the low binding energy of *cis*-N_2O_2 of about (700 ± 10) cm^{-1} [Eq. (9)]:[74,75]

$$cis\text{-ONNO} \rightleftharpoons 2\,NO \qquad \Delta H^{\ominus} = 8\ kJ\ mol^{-1} \tag{9}$$

N–N bond cleavage in *cis*-N_2O_2 was initiated by irradiation of the Ne/NO deposit with the light of a globar source transmitted through KBr and Si windows (400–8000 cm^{-1}). The IR photodissociation of *cis*-N_2O_2 by excitation of its predissociative modes, ν_5 (1789 cm^{-1}), $2\nu_5$ (3531 cm^{-1}) and $\nu_1+\nu_5$ (3609 cm^{-1}), has previously been studied in the gas phase[74,76] and in solid Ne matrices.[71] Accordingly, the difference spectrum shown in Figure 3b indicates a depletion of bands particularly of the most intense matrix site of *cis*-N_2O_2 (decreased transmittance) and its conversion into the vdW $(NO)_2$ dimer (increased transmittance).

Co-deposition at 6.3 K of Ne/NO (400:1) and Ne/O_2 (400:2) mixtures was shown to produce additional bands that were attributed to O_2 complexes and oxidation products of NO.[1,53] As shown in Figure 4, the $ON{\cdot}O_2$ complex produced under these conditions displays a prominent and slightly split N=O stretching band at 1871.9 cm^{-1} that strongly increases with the relative amount of O_2 in the deposit. This band also corresponds to both a weak O=O stretching-band doublet located at 1540.0 and 1531.1 cm^{-1} (free oxygen isolated in solid Ne at 1554.6 and 1552.2 cm^{-1}), and a strong UV charge-transfer transition reported previously.[1] The small redshifts of the NO and O_2 bands upon complexation of 3 and 18 cm^{-1}, respectively, and the absence of any inter-fragment vibrations in the IR spectrum at wavenumbers ≥ 180 cm^{-1} indicate a weak linkage between the two almost unperturbed diatomic radicals.[1] The $ON{\cdot}O_2$ complex in solid Ne was subjected to mercury-arc radiation transmitted through a 260 to 400 nm band pass filter (Schott UG11) and produced the NO_3 radical, which by subsequent irradiation at $\lambda \geq 495$ nm is destroyed with the concomitant regeneration of the $ON{\cdot}O_2$ complex.[1]

By comparing Figure 3 with Figure 4, apparently no additional bands can be attributed to the expected O_2 complex with *cis*-N_2O_2. However, the strong depletion of the $(NO)_2$ dimer bands relative to those of the NO monomer with increasing concentration of O_2 indicates a rapid thermal reaction of the $(NO)_2$ dimer species with O_2. This is evident from the IR spectra of the $Ne/O_2/NO$ deposits, which revealed additional weak absorptions due to *trans*-$ONONO_2$ and *sym*-N_2O_4 (not shown in Figure 4). It is not expected that the thermal oxidation of the $(NO)_2$ dimer species has already taken place in the gas phase prior to their condensation, because 1) *trans*-$ONONO_2$ is not a stable species in the gas phase at ambient temperatures and the relative amount of NO_2 monomer among the oxidation products is quite low, and 2) this reaction is known to be much faster in the condensed phase, proceeding very likely during the deposition of the $Ne/O_2/NO$ mixtures just before the deposit is cooled down to a rigid matrix. This conclusion is supported by the previous observation of a thermal reaction between 2 NO and O_2 in solid O_2[21] and Ar matrices[36] at temperatures ≥ 30 K. The depletion of the *cis*-N_2O_2 bands and the concomitant formation of the two N_2O_4 species strongly indicate that the *cis*-$N_2O_2{\cdot}O_2$ complex might be the precursor of the fast thermal reaction. However, because the activation

energy for diffusion of NO monomers in solid matrices might be similar or even lower than that of the dissociation of *cis*-N_2O_2,[65] and because the mobility of NO in annealed matrices is well evidenced,[36,65,70,77] N_2O_4 may also be formed by the reaction of thermally activated NO monomers with the ON·O_2 complex. In both cases, N_2O_4 formation competes with NO dimerisation.

cis-N_2O_2 was found to be rather stable in solid O_2 at 13 K,[21] and the formation of a *cis*-N_2O_2·O_2 complex by UV photofragmentation of *sym*-N_2O_4 in solid Ne proves that this complex can be stabilised at sufficiently low temperatures. The NO stretches of *cis*-N_2O_2·O_2 in solid Ne (1867.1, 1865.6 cm^{-1}; 1780.1, 1777.3 cm^{-1}) appeared only slightly shifted from those observed for *cis*-N_2O_2·in a Ne matrix (1866.7, 1865.5 cm^{-1} (ν_1); 1780.2, 1778.5 cm^{-1} (ν_5)), which indicated only a very weak interaction between *cis*-N_2O_2 and O_2. Co-deposition of Ne/NO and Ne/O_2 mixtures allows only for a small fraction of the *cis*-N_2O_2 molecules to be isolated in a site together with an O_2 molecule. The IR bands of the *cis*-N_2O_2·O_2 complexes formed by this way are not fully resolved from those of free *cis*-N_2O_2. However, upon increasing the relative amount of O_2, a shoulder blueshifted from ν_1 at 1867.1 cm^{-1} and a more prominent band redshifted from ν_5 at 1777.3 cm^{-1} grow, both of which can be attributed to the O_2 complex by comparison with the band position obtained from UV photofragmentation of *sym*-N_2O_4 in solid Ne. The vdW $(NO)_2$ dimer band at 1857.9 cm^{-1} revealed no such complexation shift in the presence of O_2, which indicated that this species does not form a stable complex with O_2 in solid Ne and, probably, will rapidly react with O_2 molecules in nearest-neighbour positions to form *trans*-$ONONO_2$ and *sym*-N_2O_4. Support for this conclusion comes from the IR photolysis experiments described in the following section.

Photolysis of Ne/NO matrices in the presence of O_2: Radiation from a globar source (400–8000 cm^{-1}) did not affect the bands due to the ON·O_2 complex (1871.9 cm^{-1}), whereas that of the vdW $(NO)_2$ dimer (1857.9 cm^{-1}) increased slightly and those attributed to the *cis*-N_2O_2·O_2 complex decreased strongly with a concomitant increase in intensity of all absorptions arising from *trans*-$ONONO_2$ and *sym*-N_2O_4. We noticed that the bands of these two N_2O_4 species grow simultaneously during irradiation to about three times the intensity of the initial deposit.

The IR spectrum of the deposit obtained after 10 min of IR irradiation is shown in Figure 5 (trace b, transmittance (T) scale) for three different wavenumber regions and compared to the reference spectrum obtained from the UV photolysis ($\lambda = 260$–400 nm) of *sym*-N_2O_4 (trace a, absorbance (A) scale). The spectra shown in trace c were obtained from experiments using $^{18}O_2$ in place of $^{16}O_2$. A complete list of the absorptions observed after exposure of the Ne/$^{16}O_2$/NO and Ne/$^{18}O_2$/NO samples to the IR radiation and their tentative assignment is given in Table S1 (in the Supporting Information). IR irradiation of the Ne/$^{18}O_2$/NO deposits did not change the positions of bands arising from NO and $(NO)_2$ dimers compared to the experiment using $^{16}O_2$, but those attributed to the NO·O_2 complex (1540.1, 1531.2 cm^{-1}) exhibited the expected $^{16/18}O$ isotopic shift of about -87 cm^{-1} of the O_2 stretching band.

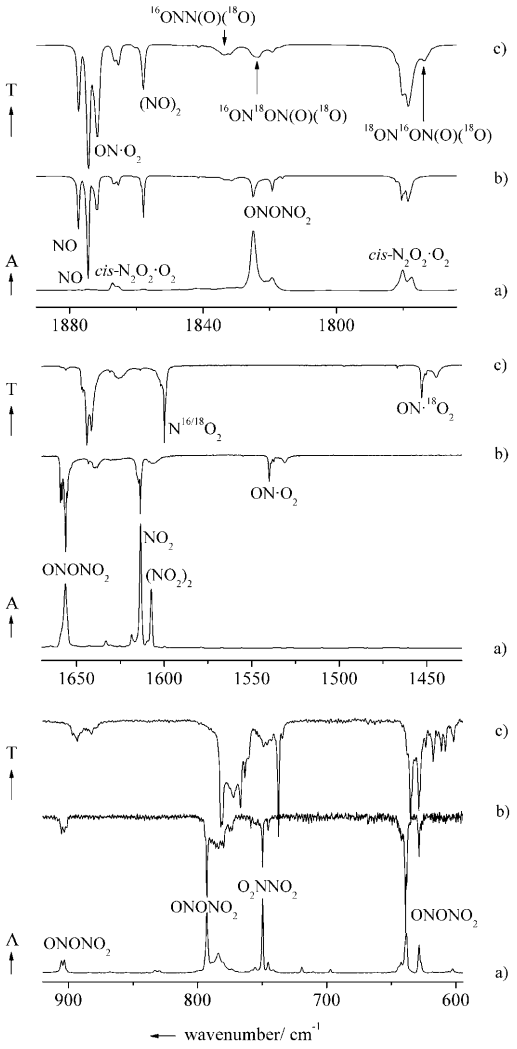

Figure 5. Bands of various nitrogen oxide species isolated in solid Ne at 6.3 K: a) *sym*-N_2O_4 exposed to filtered mercury-arc radiation, 260–400 nm; b) Ne/NO = 400 co-deposited with Ne/$^{16}O_2$ = 200, and exposed to IR radiation (400–8000 cm^{-1}); c) Ne/NO = 400 co-deposited with Ne/$^{18}O_2$ = 100, and exposed to IR radiation (400–8000 cm^{-1}).

The appearance of only one NO_2 monomer band at 1599.9 cm^{-1} in the $^{18}O_2$ experiment (Figure 5, trace c) indicates the selective formation of the mixed $N(^{16}O)^{18}O$ isotopologue.[67] Dimerisation of $N(^{16}O)^{18}O$ yielded di-^{18}O-substituted *sym*-N_2O_4 (D_{2h}). The two ^{18}O atoms may adopt the *syn* or the *anti* positions in the planar O_2N–NO_2 molecule, and the centre of symmetry is retained only for the latter one. The fundamental bands of these mixed $^{16/18}O$ isotopomers appeared at 1738.1 (b_{2u}), 1233.5 (b_{3u}, not shown in Figure 5), and 737.4 cm^{-1} (b_{3u}, Figure 5, trace c). These bands revealed no resolved $^{16/18}O$ isotopic splitting, which indicated only a weak coupling between the two weakly

linked NO_2 groups in this molecule. The weak out-of-plane deformation ν_7 (b_{1u}) was not observed in the $^{18}O_2$ experiment.

From the spectra shown in Figure 5, and from the observation that solely the mixed isotopologue $N(^{16}O)^{18}O$ was formed in the reaction of *cis*-N_2O_2 + $^{18}O_2$, we conclude that asymmetric dimerisation of $N(^{16}O)^{18}O$ produced four isotopomers of *trans*-$ONONO_2$ (Scheme 1). The $^{16/18}O$ isotopic splitting pattern will be discussed below.

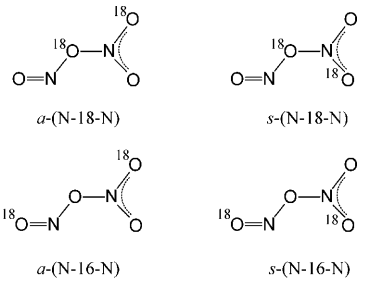

Scheme 1. Isotopomers of *trans*-$ONONO_2$ formed by the asymmetric dimerisation of $N(^{16}O)^{18}O$.

After the unambiguous assignment of the bands due to *trans*-$ONONO_2$, *sym*-N_2O_4 and the NO_2 monomer, only a few additional broad features remained unassigned. These features were located at about 1832 (m), 1639 (m), 1606 (m) and 1303 cm^{-1} (m). From the experiment using the $^{18}O_2$ sample, the corresponding shifted band positions were obtained at 1833 (m, br), 1626 (m, br) and 1280 cm^{-1} (m), but the ^{18}O-substituted carrier of the broad band at about 1606 cm^{-1} was not formed in this experiment.

These additional bands also appeared upon exposure of $Ne/O_2/NO$ matrices to UV irradiation ($\lambda = 260$–400 nm),[53] in which the broad band observed at 1606 cm^{-1} on IR photolysis was replaced by a much sharper band at 1607.5 cm^{-1}. This band is assigned to the $(NO_2)_2$ dimer complex already detected in the N_2O_4 photolysis experiment. The remaining three bands are attributed to *asym*-N_2O_3, $ONNO_2$,[42,78] for the following reasons: 1) In the presence of NO the dimerisation of NO_2 competes with the formation of $ONNO_2$ [Eq. (10)]:

$$NO + NO_2 \rightarrow ONNO_2 \qquad \Delta H^{\ominus} = -41\ kJ\,mol^{-1} \tag{10}$$

2) The corresponding features in the spectra of the photolysis products are very close to band positions observed for an authentic sample of $ONNO_2$ prepared by the co-deposition of NO and NO_2 in solid Ne: 1831.5 (s), 1830.0 (s), 1643.3 (s) and 1302.5 cm^{-1} (s). However, the reaction $2NO + O_2$ yields a NO_2 radical pair and, because only one of these NO_2 radicals can combine with NO to $ONNO_2$, the presence of the second NO_2 free radical, co-isolated in the same matrix cage, may account for the strong broadening and small frequency shifts. 3) The absence of a $N{=}^{18}O$ absorption redshifted from the feature at 1833 cm^{-1} by 46 cm^{-1} (Figure 5, trace c) supports the assignment of the bands at 1833, 1626 and 1280 cm^{-1} to $^{16}ONN(^{16}O)^{18}O$, rather than to an $ONONO_2$ species formed by asymmetric dimerisation of $N(^{16}O)^{18}O$.

Comparison with DFT and ab initio MP2 calculations: Molecular structures, infrared spectra and the $^{16/18}O$ isotopic shifts of the NO_2 monomer, *sym*-N_2O_4, *trans*-$ONONO_2$, and weakly bound $(NO_2)_2$ dimers have initially been explored computationally at the DFT B3LYP/311+G(2d) level,[79] which has been shown to give reliable predictions of the vibrational spectra of such weakly bonded nitrogen oxides.[59,80] The calculated wavenumbers for *trans*-$ONONO_2$ (C_s) given in Table 2 are similar to those reported in previous theoretical DFT and ab initio MP2 studies.[39,64,81] As a first guess, relative energies were estimated using the complete basis set CBS-QB3 method.[82] The optimised geometries and relative energies (including zero-point-energy (ZPE) correction) for the minimum structures of these species are illustrated in Figure 2. The calculated relative energies with respect to $2NO_2$ monomers for *sym*-N_2O_4 and *trans*-$ONONO_2$, -53.7 and -28.5 kJ mol^{-1}, respectively (Figure 2), agree reasonably well with experimental values [(-57.0 ± 0.3)[25] and -38 kJ mol^{-1}; Eqs. (6) and (8)].

Several weakly bound $(NO_2)_2$ dimers have been optimised at the N_2O_4 singlet potential-energy surface. The most stable one of these had C_{2h} symmetry and its structure is shown in Figure 2. This NO_2 radical pair was proposed to be a key intermediate in the nitric oxide oxidation process, formed by O–O bond homolysis of *s-cis,cis*-ONOONO [Eq. (4)].[40] At the CBS-QB3 level it is 2.4 kJ mol^{-1} higher in energy than $2NO_2$ monomer radicals (Figure 2). This is close to the CCSD(T) relative energy reported previously (+5.7 kJ mol^{-1}),[41] while the broken-symmetry (BS) DFT approach,[83] which is more appropriate to a diradicaloid system,[84] predict a reversed order of stability, $(NO_2)_2$ dimer $> 2NO_2$ (-2.4 kJ mol^{-1}, BS-B3LYP/6-311+G(2d) level).[41] Due to its centre of symmetry, only antisymmetric combinations of the N=O stretching vibrations are IR active. Its strongest band is predicted to appear redshifted from the strong NO_2 monomer band at 1613.7 cm^{-1}, and we tentatively attributed the carrier of the band at 1607.5 cm^{-1} in Figures 1 (lower trace) and 5 (trace a) to this NO_2 radical pair.

In principle, nitrosooxy (ONO–) compounds may adopt *cis* or *trans* geometries within a planar ON–OX chain. Therefore, molecular structures and the vibrational spectra of *cis*-like $ONONO_2$ have also been calculated at both the DFT B3LYP/311+G(2d)[79] and the CBS-QB3[82] levels for comparison (Tables S2–S4 in the Supporting Information). In general, The PES at the optimised geometries for the various $ONONO_2$ isomers were found to be very flat, and predicted barriers for the internal rotation of the NO_2 group around the ONO–NO_2 bond were, in agreement with previous studies on *trans*-$ONONO_2$,[64] particularly low. Consistent with these observations at least two different non-

planar geometries with similar relative energies were reported for the *cis* conformer.[39–41,81] We verified both the reported *cis*-like structures (Table S3), in which the NO_2 group is twisted out of the $O^6N^5O^4N^3$ plane by either about 36° (denoted as *cis*-$ONONO_2$ (C_1) in Figure S1 in the Supporting Information), or 90° (*cis-perp*-$ONONO_2$ (C_s) in Figure S1 (*perp* = perpendicular)). At the CBS-QB3 level *cis*- (C_1) and *cis-perp*-$ONONO_2$ (C_s) are predicted to be local minima with energies of 13.5 and 17.0 kJ mol^{-1} (Table S4) higher than trans-$ONONO_2$ (C_s).

Because of the low bonding energy especially of the *cis*-like $ONONO_2$ isomers, further calculations have been carried out using 1) spin-component scaled second-order Møller–Plesset perturbation theory[85] (SCS-MP2),[86,87] and 2) various DFT-D methods,[88,89] in which PBE,[90] B2PLYP[91] and B3LYP[79] density functionals were augmented with an empirical correction for long-range dispersion effects (Tables S6–S8 in the Supporting Information). Molecular geometries of four different isomers, *trans*-$ONONO_2$ (C_s and C_1 symmetry), *cis*- (C_1) and *cis-perp* (C_s) $ONONO_2$ (Figure S1 in the Supporting Information) were fully optimised at both the SCS-MP2 (Table S5 in the Supporting Information) and the DFT-D B3LYP (Table S8 in the Supporting Information) levels. Consistent with the CBS-QB3 method these calculations predict *trans* to be more stable than *cis* by about 10 (SCS-MP2) and 7.5 kJ mol^{-1} (B3LYP-D), respectively (Tables S5 and S8). To the contrary, the *cis-perp* (C_s) conformer was optimised at the PBE-D approach to dissociate into $2\,NO_2$ (Table S6 in the Supporting Information). Vibrational spectra obtained at the MP2 level predict unreasonable high antisymmetric NO_2 stretching frequencies and imaginary frequencies for the NO_2 torsional mode in both the *trans* (C_1) and *cis-perp* (C_s) isomers (Table S10 in the Supporting Information). On the other side, calculated geometries and frequencies at the B3LYP-D level for *trans*- (C_s) and *cis*- (C_1) $ONONO_2$ (Tables S8 and S11 in the Supporting Information) are very similar to those obtained without dispersive correction (Table 2; Tables S2 and S3). These results are in accord with recent observations that the B3LYP method reproduces N–O bonds lengths in covalent nitrates and nitrites fairly well.[92,93] In both conformers, *trans*- (C_s) and *cis*- (C_1) $ONONO_2$, the two central N–O bond lengths are predicted to be considerably different, and N^3–O^4 is always found to be shorter than O^4–N^5 (Figure 2, Tables S3–S8). For *cis-perp*-$ONONO_2$ (C_s) the B3LYP/311+G(2d) approach revealed one imaginary frequency (Table S3), whereas both the recommended B3LYP/AUG-cc-pVQZ and B3LYP-D/def2-QZVP methods, using large basis sets, predicted a true minimum with only a marginal difference between the two central N–O bond lengths (Table S8).

For a planar O=N-OX chain the *cis* conformer usually exhibits higher N–O and lower N=O stretching vibrations than the *trans* isomer.[94,95] This observation can be rationalised by the anomeric effect, that is, delocalisation of the lone pairs at the central nitrogen and oxygen atoms in the *cis* conformer, strengthening the central N–O bond on account of the terminal O–X and O–N bonds, respectively.[96,97] While this feature is reminiscent for *cis-perp* (C_s) with a planar N^3-O^4-N^5-O^6 chain, the spectrum of non-planar *cis*-$ONONO_2$ (C_1) is rather different (Table S11 in the Supporting Information). The latter reveals the weakest interaction between the N=O moiety and the O_2N–O group and its N=O stretching frequency is predicted to be only slightly redshifted from that of the NO monomer. This in part results from the loss of π conjugation in the non-planar O=N-O-N unit.

Mechanism of the UV photolysis of *sym*-N_2O_4 isolated in a Ne matrix: The photochemistry of *sym*-N_2O_4 has been studied intensively in the gas phase[26,98] and adsorbed on metal substrates.[99] Despite the fact that the primary photoproducts of a molecule isolated in a rare-gas matrix are, in principle, similar to those in the gas phase, the final products that are observed in matrix-isolation experiments often differ from those obtained for gas phase or adsorbed species. This is because secondary reaction products are often formed within the matrix cage. Thus, whereas the photolysis of gaseous NO_2 with light <398 nm (300 kJ mol^{-1}) is known to produce NO and O atoms [Eq. (11)],[100] the intensity of the NO_2 monomer band in solid Ne remained unchanged under the UV photolysis, because of the rapid NO + O recombination and energy dissipation within the matrix cage.

$$NO_2 \rightleftharpoons NO\ (X\ ^2\Pi_{1/2}) + O\ (^3P_2) \qquad \Delta H^\ominus = 307\ \text{kJ mol}^{-1} \tag{11}$$

sym-N_2O_4 exhibits two weak absorption bands centred at 345 nm ($^1B_{2u} \leftarrow {}^1A_g$) and about 260 nm ($^1A_u \leftarrow {}^1A_g$),[98,101] and the primary process observed for the gas-phase photolysis at these wavelengths is its dissociation into two NO_2 radicals. By considering the photon energies used in our experiment, 260 to 400 nm (460 to 299 kJ mol^{-1}, respectively), the bond-dissociation energy of *sym*-N_2O_4 (57.0 kJ mol^{-1}),[25] and the two first electronic excited states of NO_2, A $^2B_2$ and B $^2B_1$, lying at 116.2 and 176.5 kJ mol^{-1}, respectively, above the ground state,[26] the photolysis can, in principle, produce any combination of the X, A and B states in the NO_2 photofragments [Eqs. (12)–(14)]:

$$sym\text{-}N_2O_4 \rightleftharpoons 2\,NO_2\ (X\ ^2A_1) \qquad \Delta H^\ominus = 57\ \text{kJ mol}^{-1} \tag{12}$$

$$sym\text{-}N_2O_4 \rightleftharpoons NO_2\ (X\ ^2A_1) + NO_2{}^*\ (A\ ^2B_2) \qquad \Delta H^\ominus = 173\ \text{kJ mol}^{-1} \tag{13}$$

$$sym\text{-}N_2O_4 \rightleftharpoons NO_2\ (X\ ^2A_1) + NO_2{}^*\ (B\ ^2B_1) \qquad \Delta H^\ominus = 234\ \text{kJ mol}^{-1} \tag{14}$$

Previous studies of the 351 nm photolysis have shown that the major photodissociation process in the gas phase is described by Equation (13),[26] and for *sym*-N_2O_4, isolated in a solid Ne matrix, these primary-formed radicals are expected to recombine rapidly to form a N–O linkage, because unlike

the ground state, in the electronic excited B states of NO_2 the unpaired electron is primarily localised at the O atoms [Eq. (15)].

$$NO_2\ (X\ ^2A_1) + NO_2{}^*\ (A\ ^2B_2) \rightarrow \textit{trans}\text{-}ONONO_2 \qquad \Delta H^{\ominus} \approx -154\ kJ\ mol^{-1} \tag{15}$$

The presence of *cis*-$N_2O_2{\cdot}O_2$ among the photolysis products indicates N–O bond fission upon the photolysis. NO radicals might be formed in a secondary photolysis reaction from primary-formed NO_2 according to Equation (11), and subsequent abstraction of an oxygen atom from NO_2 by the co-isolated O atom in the same cage may produce *cis*-$N_2O_2{\cdot}O_2$ according to Equation (16):

$$NO_2\ (X\ ^2A_1) + NO\ (X\ ^2\Pi_{1/2}) + O\ (^3P_2) \rightarrow \textit{cis}\text{-}N_2O_2 + O_2\ (X\ ^3\Sigma_g^-) \qquad \Delta H^{\ominus} = -200\ kJ\ mol^{-1} \tag{16}$$

Formation of NO and NO_2 was indeed shown to be the primary process in the UV photolysis ($\lambda = 400$ nm) of multilayer N_2O_4 adsorbed on Au(111),[99] and for N_2O_4 deposited on ice at wavelengths of 248 and 351 nm.[23] Because the threshold energy for the N–O dissociation might be even lower for the direct photolysis of *sym*-N_2O_4, alternative reaction sequences leading to NO should be considered [Eqs. (17)–(20)]:

$$\textit{sym}\text{-}N_2O_4 \rightarrow \textit{asym}\text{-}N_2O_3 + O\ (^3P_2) \qquad \Delta H^{\ominus} = 323\ kJ\ mol^{-1} \tag{17}$$

$$\textit{asym}\text{-}N_2O_3 + O\ (^3P_2) \rightarrow \textit{cis}\text{-}N_2O_2 + O_2\ (X\ ^3\Sigma_g^-) \qquad \Delta H^{\ominus} = -160\ kJ\ mol^{-1} \tag{18}$$

$$\textit{sym}\text{-}N_2O_4 \rightarrow NO_2\ (X\ ^2A_1) + NO\ (X\ ^2\Pi_{1/2}) + O\ (^3P_2) \qquad \Delta H^{\ominus} = 364\ kJ\ mol^{-1} \tag{19}$$

$$NO_2\ (X\ ^2A_1) + O\ (^3P_2) \rightarrow NO\ (X\ ^2\Pi_{1/2}) + O_2\ (X\ ^3\Sigma_g^-) \qquad \Delta H^{\ominus} = -192\ kJ\ mol^{-1} \tag{20}$$

The escape of photolytically generated O atoms out of the matrix cage has been reported[77,102,103] but appears to be negligible in the present study. To the contrary, the formation of NO_3 radicals upon the near-UV irradiation of the Ne matrix seems likely [Eqs. (21)–(23)]:

$$NO_2\ (X\ ^2A_1) + O\ (^3P_2) \rightarrow NO_3\ (X\ ^2A_1) \qquad \Delta H^{\ominus} = -211\ kJ\ mol^{-1} \tag{21}$$

$$\textit{trans}\text{-}ONONO_2 \rightarrow NO_3\ (X\ ^2A_1) + NO\ (X\ ^2\Pi_{1/2}) \qquad \Delta H^{\ominus} \approx 133\ kJ\ mol^{-1} \tag{22}$$

$$NO\ (X\ ^2\Pi_{1/2}) + O_2\ (X\ ^3\Sigma_g^-) \rightarrow NO_3\ (X\ ^2A_1) \qquad \Delta H^{\ominus} = -19\ kJ\ mol^{-1} \tag{23}$$

Indeed, we detected traces of NO and NO_3 radicals by their IR and visible spectra, respectively, among the photoproducts of *sym*-N_2O_4 isolated in a Ne matrix. However, for a NO and NO_3 radical pair co-isolated in the same matrix cage, their rapid recombination to form *trans*-$ONONO_2$ is expected. Thus, although the photochemistry of *sym*-N_2O_4 isolated in a solid Ne matrix appears to be rather complex, only *trans*-$ONONO_2$, the *cis*-$N_2O_2{\cdot}O_2$ complex, and a weakly bound $(NO_2)_2$ dimer complex were proved to be formed as stable photoproducts. The photofragments NO + NO_3, each with an unpaired electron, can be prevented from their recombination only when they exist in different matrix cages, separated by a marginal reorganisation of their matrix environment, and as will be discussed below, the *cis*-$N_2O_2{\cdot}O_2$ complex can exist only when its internal energy is lower than that required for its N–N bond homolysis. Detection of the $N_2O_2{\cdot}O_2$ complex among the photolysis products indicates that excited photofragments are quickly quenched in the solid matrix.

Vibrational spectrum of nitroso nitrate: Large discrepancies in the experimental vibrational frequencies have been reported for $ONONO_2$ produced under different experimental conditions,[59] which may be attributed to 1) a high degree of conformational flexibility;[64] 2) its large dipole moment ($\mu \approx 2.6$ D),[61] suggesting strong interactions with polar environments; and 3) the assumed co-existence of three isomeric species: *trans*- and *cis*-$ONONO_2$ with respect to the nitrosooxy ON–O single bond and ionic nitrosonium nitrate, $NO^+NO_3^-$.[15,24,43–45]

Indeed, in former matrix-isolation studies both *cis*- and *trans*-$ONONO_2$ (denoted as D′ and D, respectively) were tentatively assigned.[20] The predicted spectra for *trans*- (Table 2) and *cis*-like $ONONO_2$ (Table S2 in the Supporting Information) reveal substantial differences. The worse agreement between the experimental and the calculated spectrum for the *cis* conformers (Table S2) supports the assignment given in Table 2 to *trans*-$ONONO_2$. The preferred formation of *trans*- over *cis*-$ONONO_2$ is also consistent with their predicted thermochemical stability *trans* > *cis*.

The observed band positions for *trans*-$ONONO_2$ in solid Ne agree well with previous results obtained in solid O_2 and Ar.[18,20] Most of the frequency differences are a few cm^{-1}, except for the antisymmetric NO_2 stretch, observed at 1656.2 cm^{-1} in solid Ne, which is redshifted by about 12 cm^{-1} in O_2 and in Ar matrices (Table 3).[18,20] On the other hand, the substantial shifts of the reported frequencies observed previously in solid N_2,[22] as well as for the Raman bands in solid Ne[17] (Table 3), cannot solely be explained by matrix shifts. The frequency discrepancies between our data and those of the former Raman study may be due to the much higher concentration used previously.[17]

The far-IR bands < 700 cm^{-1} of *trans*-$ONONO_2$ reveal significant site/conformational splitting. The band ν_6 is assigned to a doublet at 639.0 and 628.6 cm^{-1} (Figure 1, lower trace), however, only the high-frequency site is listed in Tables 1 and 3 because our previous studies[1] revealed a preferential

Table 3. Comparison of observed fundamental band positions [cm^{-1}] of *trans*-$ONONO_2$ in decreasing order and in different solid matrices.

Ne[a]	Ne[b]	Ar[c]	O_2[d]	N_2[e]
1824.9	1806	1827.9	1829	1861
1656.2	1635	1644.0	1645	1628
1293.2	1295	1290.5	1291	1279
903.3	–	903.3	905	911
792.9	783	786.9	783	792
784.1	–	–	–	–
639.0	622	–	642	647
488.2	–	–	488	–
306.0	–	–	304	–

[a] Ne matrix. This work. [b] Raman, Ne matrix (see text). Ref. [17]. [c] Ar matrix. Ref. [18]. [d] O_2 matrix. Ref. [20,21]. [e] N_2 matrix (see text). Ref. [22].

occupation of this site after exposure of the samples to radiation in the UV and Vis range. The far-IR bands around 490 and 310 cm^{-1} both exhibit a very rich matrix splitting pattern composed of several closely spaced absorptions. As matrix site occupancy depends on the experimental conditions, subsequent photolysis and annealing experiments have revealed a preferential occupation of the corresponding low frequency sites, which are associated with absorptions at 488.2 and 306.0 cm^{-1}. One additional feature with a similar behaviour on photolysis as the fundamentals of *trans*-$ONONO_2$ appeared at 1273.7 cm^{-1}. This band is associated with a combination band of *trans*-$ONONO_2$ (488 + 792.9 = 1281 cm^{-1}).

Compared to previous work, we completed the list of fundamentals of *trans*-$ONONO_2$ in the range >250 cm^{-1} and carried out $^{16/18}O$-labelling experiments. The two oxygen atoms of the terminal NO_2 group are not equivalent and a mono-^{18}O-substituted oxygen in the $N(^{16}O)^{18}O$ moiety may adopt the *syn* or the *anti* position relative to the N=O substituent (Scheme 1). Thus, asymmetric dimerisation of $N(^{16}O)^{18}O$ to *trans*-nitroso nitrate results in four different isotopomers: *s*-(N-16-N), *a*-(N-16-N), *s*-(N-18-N) and *a*-(N-18-N) (Scheme 1). Experimental and calculated $^{16/18}O$ isotopic shifts $\Delta\nu(^{16/18}O)$ of these isotopomers are compiled in Table 4.

The ^{18}O=N stretching vibration ν_1 of the N-16-N isotopomers is obscured by ν_5 of *cis*-N_2O_2. Its $^{16/18}O$ isotopic shift, $\Delta\nu(^{16/18}O)$, was estimated from a less-occupied matrix site associated with a weak band at 1773.6 cm^{-1} (Figure 5, trace c) to be about 45.7 cm^{-1}, which is close to the corresponding value of 46.4 cm^{-1} observed for the related molecule $^{16/18}ONNO_2$ isolated in solid Ar.[78] The high O=N stretching frequency, and the small contribution from the bridging O^4 atom to the $^{16/18}O$ isotopic shift of this mode (about 1.0 cm^{-1}, Table 4) revealed only weak interactions between the O=N and the O_2N-O^4 moieties in *trans*-$ONONO_2$.

The observed shifts $\Delta\nu(^{16/18}O)$ for ν_2 (1656.2 cm^{-1}) and ν_3 (1293.2 cm^{-1}) are close to those for the antisymmetric NO_2 stretch of the $^{16}ON^{18}O$ monomer ($\Delta\nu(^{16/18}O) = 13.8$ cm^{-1}), and the symmetric NO_2 stretch of *sym*-N_2O_4 (27.0 cm^{-1}) in solid Ne, respectively. Of these, only the ν_2 band reveals a splitting in the ^{18}O experiment of approximately 2.5 cm^{-1} (Figure 5, trace c).

For the vibrations ν_4 (903.3 cm^{-1}), ν_5 (792.9 cm^{-1}) and ν_6 (639.0 cm^{-1}), the N-18-N isotopomers exhibit considerably larger $\Delta\nu(^{16/18}O)$ shifts than the N-16-N species. This indicates a substantial contribution by $^{16/18}O$ substitution of the bridging O^4 atom to these particular modes, which are further split by ^{18}O monosubstitution of either the *syn* or the *anti* O atoms of the NO_2 group. A large splitting of the ν_4 band upon ^{18}O substitution is consistent with its assignment to the O_2N-O^4 stretching fundamental (Table 2), however, because of the appearance of different matrix sites and the low intensity of these bands, only an averaged isotopic shift over distinct matrix sites for the *syn* and *anti* isotopomers is given in Table 4.

The $^{16/18}O$ isotopic pattern of ν_5 (792.9 cm^{-1}, a′) is actually very similar to that of ν_4 (Table 4). This may indicate vibrational mixing between these two modes. The assignment of ν_5 to a mixed O_2N-O^4 stretch/NO_2 bend vibration (Table 2) is consistent with the observation that the NO_2 bending modes of nitro compounds usually appear in a narrow range around 800 cm^{-1}.[42] The $^{16/18}O$ isotopic patterns of ν_5 and ν_{10} (784.1 cm^{-1}, a″) almost coincide, and as the barrier for the ONO–NO_2 torsion was found to be rather low,[59] one cannot exclude a slight tilt of the NO_2 group out of the molecular plane, which, in addition, might result in a vibrational mixing between ν_5 and ν_{10}, at least for the N-18-N species.

The confusing $^{16/18}O$ isotopic pattern of ν_6 is in accord with the predicted one (Table 4), when the pronounced site splitting of this band of about 10 cm^{-1} is considered. The absorptions due to the N-18-N species appeared to be much weaker than those of the N-16-N isotopomers located at 635.3

Table 4. $^{16/18}O$ isotopic shifts $\Delta\nu(^{16/18}O)$ [cm^{-1}] of various isotopomers of *trans*-$ONONO_2$ relative to the natural compound observed in solid Ne and compared to calculated isotopic shifts.[a]

ν_i	*a*-(N-18-N)	*s*-(N-18-N)	*a*-(N-16-N)	*s*-(N-16-N)	Completely ^{18}O-substituted[b]
ν_1	1.0 (0.7)	1.0 (0.8)	≈45.7 (49.8)	≈45.7 (49.9)	–
ν_2	14.6 (15.3)	12.1 (13.0)	14.6 (14.9)	12.1 (12.7)	–
ν_3	25.0 (25.0)	25.0 (25.4)	25.0 (24.5)	25.0 (24.7)	–
ν_4	21.1[c] (22.9)	21.1[c] (27.5)	10.0[c] (7.2)	10.0[c] (12.1)	–
ν_5	26.0[d] (16.8)	29.4[d] (16.8)	10.8[d] (14.0)	12.0[d] (14.0)	–
ν_6	27.8 (30.0)	21.5 (23.1)	10.3 (10.7)	3.8 (4.0)	32.0 (34.2)
ν_7	– (6.8)	– (12.0)	– (7.9)	– (13.1)	18.3 (19.6)
ν_8	– (5.8)	– (2.9)	– (7.1)	– (3.7)	10.3 (9.6)
ν_{10}	11.0[c] (6.0)	11.0[c] (6.0)	11.0[c] (4.0)	11.0[c] (4.0)	–

[a] For the notation of the isotopomers see Scheme 1. The listed $\Delta\nu(^{16/18}O)$ values have negative signs. Calculated $^{16/18}O$ isotopic shifts [cm^{-1}] at the DFT B3LYP/311+G(2d) level are given in parentheses. [b] $^{16/18}O$ isotopic shifts [cm^{-1}] of the full ^{18}O-substituted isotopologue from ref. [1]. [c] Isotopic shift averaged over distinct matrix sites of the corresponding *syn* and *anti* isotopomers. [d] See text.

and 628.8 cm^{-1} (Figure 5, trace c). However, unlike the two N-16-N species, for which a single site is most dominant, the bands attributed to the two N-18-N isotopomers seem to be split into a 1:1 doublet, separated by about 9.5 cm^{-1}. Movement of both, the bridging-O^4 and the *anti*-O^2 atoms are mainly involved in this mode, which is described as a $O^2N^3O^4$ bend in Table 2.

Due to the multiple matrix splittings of the far-IR bands ν_7 (around 480 cm^{-1}) and ν_8 (about 310 cm^{-1}) their assignment to different isotopologues of the mixed $^{16/18}O$ species becomes difficult and has not been attempted. In our previous far-IR study, devoted to the NO_3 radical,[1] spectra of the *full* ^{18}O isotopologue of *trans*-$ONONO_2$ have been obtained, and the corresponding $^{16/18}O$ isotopic shifts of ν_6, ν_7 and ν_8 are compiled in Table 4. Furthermore, both the different labelling $N^{18}O+O_2$ and $NO+{}^{18}O_2$ were shown to yield the same four isotopomers of *trans*-$ONONO_2$ (Scheme 1) by irradiation of the corresponding deposits.[1]

The most intriguing features of the vibrational spectrum of *trans*-$ONONO_2$ are the striking differences between the two central N–O single bonds. The computationally predicted very different bond lengths (Figure 2) correspond to a large frequency difference between the two N–O stretching modes ν_4 (903.3 cm^{-1}) and ν_8 (about 310 cm^{-1}), respectively (Table 2). For comparison, the related N–O modes of O_2N-O-NO_2 (N_2O_5) with two equal and intermediate N–O single bonds (exptl: 1.498 Å)[29,104] are predicted at 381 and 344 cm^{-1}[29,104] (exptl, Ar matrix: 344 cm^{-1}).[105] As has already been pointed out,[39] the thermochemistry of *trans*-$ONONO_2$ does not correspond to these bond-length differences, since, on energetic grounds the *shorter* O_2N^3–O^4 bond breaks upon dissociation and $2NO_2$ radicals are formed [$\Delta H^{\ominus} \approx 38$ kJ mol^{-1}; Eq. (8)] rather than NO and NO_3 [$\Delta H^{\ominus} \approx 133$ kJ mol^{-1}; Eq. (22)].

We found no evidence for the existence of a *cis*-$ONONO_2$ conformer. For comparison we refer to the most complete set of frequencies reported for this isomer,[20] also listed in Table S2 in the Supporting Information. The band at 1889–1899 cm^{-1} attributed to its N=O stretching vibration exhibits a considerable blueshift from the NO monomer line. Such high-frequency N=O fundamentals are clearly outside the range expected for nitroso compounds,[42] but have been observed recently for complexes of NO with Lewis acids.[106,107] We are thus inclined to offer an alternative assignment of the conflicting spectrum to a complex of *trans*-$ONONO_2$ and probably H_2O. It is believed that nitroso nitrate in the presence of water ionises to $NO^+NO_3^-$. Although there is so far no direct evidence for this conversion, reported frequencies for a molecular nitroso nitrate in the presence of ice on a Au(111) surface at 183 K[24] may support this tentative assignment (Table S2 in the Supporting Information). Auto-ionisation and hydrolysis of N_2O_4 species is supposed to contribute to atmospheric HONO and has attracted the interest of recent laboratory[63,108] and computational studies,[59,109] however, more experimental and computational work is necessary to elucidate this important feature of nitroso nitrate.

Implications for the NO oxidation mechanism: IR photodissociation ($\lambda = 1.25$–16.7 μm) of the N–N bond in the *cis*-$N_2O_2{\cdot}O_2$ complex, isolated in solid Ne, produced both *trans*-$ONONO_2$ and *sym*-N_2O_4 by the proposed reaction sequence shown in Equations (2) to (4) and subsequent rearrangement of the initially formed $(NO_2)_2$ radical pair according to the proposed mechanism outlined in Scheme 2.

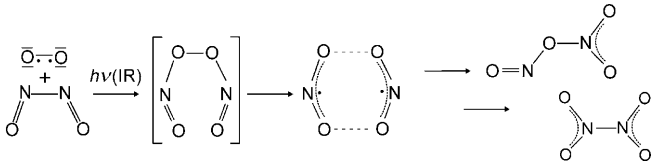

Scheme 2. Proposed mechanism for the rearrangement of the *cis*-$N_2O_2{\cdot}O_2$ complex to *trans*-$ONONO_2$ and *sym*-N_2O_4.

Considering the fast quenching evidenced for excited matrix-isolated species, the activation barrier of any step of this reaction sequence is expected not to be higher than a few kJ mol^{-1}, and the energy for the N–N homolysis of the *cis*-$N_2O_2{\cdot}O_2$ complex may probably provide the rate-determining step along this low-energy pathway. This is supported by the previously determined activation energy of $\Delta H^{\#} \approx 5$–6 kJ mol^{-1} and the kinetic $^{14/15}N$ isotopic effect of the pseudo-first-order rate constant $^{14}k/^{15}k = 1.55$ at 13 K for the thermal reaction of *cis*-N_2O_2 in solid O_2.[35]

The absence of the proposed peroxide intermediate ONOONO in the final reaction products is not quite unexpected. Apart from ONOOH,[110,111] previous studies in search of related nitroso peroxides ONOOX with X = CH_3[112] and Cl[113,114] appear to be unsuccessful. These peroxides generally feature low bond-dissociation energies and unusually low barriers for the O–O bond homolysis as well, and these properties were shown to reveal a strong conformational dependence.[40,115] Cleavage of the O–O bond was found to be much more feasible for those isomers, which exhibit the *s-cis* conformation with respect to the ON–OO bond, whereas the *trans* conformers were predicted first to isomerise prior to O–O bond dissociation. The origin of these differences is due to a large stabilisation that the O-N=O fragment undergoes in the bond-breaking transition state for the *cis* isomer.[40,115] Cleavage of the O–O bond in the *trans* conformer is predicted to yield a high-energy oxygen-centred radical (NO_2* in the A $^2B_2$ state),[40] whereas the *cis* conformer yields ground-state NO_2 radicals. The involvement of the nitrogen lone pair in the O–O bond-breaking process for the *cis* but not for the *trans* isomer may be visualised in terms of $n(N) \rightarrow \sigma^*(OO)$ orbital interaction, which lowers the O–O dissociation energy and reduces the activation barrier due to a $^2B_2$–$^2A_1$ state correlation in the corresponding transition state. To account for the proposed negligible reaction barrier for the rearrangement of the *cis*-$N_2O_2{\cdot}O_2$ complex into the N_2O_4 species, we can assume that the *cis,cis*-ONOONO isomer was formed upon IR irradiation of the matrix-isolated *cis*-$N_2O_2{\cdot}O_2$ complex due to geo-

metric constraints. This peroxide rapidly decomposes into two ground-state NO_2 radicals with an activation energy for the O−O homolysis reduced by the amount of the twofold stabilisation energies of both of the initially formed O-N=O fragments.[40]

The presence of the weakly bound $(NO_2)_2$ complex among the photolysis products indicates that its rearrangement to *trans*-$ONONO_2$ is not barrier free. Furthermore, the formation of four different ^{18}O isotopomers of *trans*-$ONONO_2$ in the experiment using labelled $^{18}O_2$ indicates its formation via a ground-state $N(^{16}O)^{18}O$ radical pair rather than its formation by a concerted ONOONO decomposition, as has been proposed recently.[40] By the same reasoning also the supposed involvement of excited NO_2* ($A\ ^2B_2$) radicals,[40] formed by the decomposition of the dinitroso peroxide, in the formation of *trans*-$ONONO_2$ can be ruled out, as in these cases only two *trans* isotopologues with a bridging ^{18}O atom would have been formed. This follows from the negligible reaction barrier and the geometric constraint within the matrix cage, which does not allow for a considerable reorientation of the electronically excited NO_2* radical. Thus the weakly bound $(NO_2)_2$ complex is shown to be an intermediate in the formation of *trans*-$ONONO_2$ rather than a side product. The concomitant formation of *sym*-N_2O_4 under these conditions is reasonable due to the weakly bound nature of this dimer and the known barrier-free dimerisation of $2\,NO_2$ to *sym*-N_2O_4.[29] Based on the high predicted barrier for the one-step thermal isomerisation of *trans*-$ONONO_2$ into *sym*-N_2O_4[41,59–61] this process is unlikely to occur under the matrix-isolation conditions.

Previous calculations on the $(NO_2)_2 \rightarrow$*trans*-$ONONO_2$ rearrangement gave insight into the asymmetric dimerisation of NO_2.[41] These calculations suggest a smooth transition from the weakly bound $(NO_2)_2$ radical pair to *cis*-like $ONONO_2$ and its subsequent isomerisation into *trans*-$ONONO_2$ by rotation of the terminal NO_2 and NO groups around the central N−O bonds. Computed barriers for the $(NO_2)_2 \rightarrow$*cis*-$ONONO_2$ and *cis*-$ONONO_2 \rightarrow$*trans*-$ONONO_2$ rearrangements amount to 15.7 (1.3) and 0.8 $kJ\,mol^{-1}$ at the CCSD(T)/aug-cc-pVDZ (BS-B3LYP/6-311+G(2d)) levels, respectively.[41] However, these calculations failed to locate a low-energy transition state for the $(NO_2)_2 \rightarrow$*sym*-N_2O_4 rearrangement.

The involvement of NO_3 radicals in the NO oxidation pathway was considered in former studies as well.[37,38] The present results rule out this possibility, as this would lead to a $^{16/18}O$ randomisation in the experiment using $^{18}O_2$. Thus, although the present work reinforces the recently predicted overall reaction scheme for the rearrangement of the *cis*-$N_2O_2{\cdot}O_2$ complex,[39–41] modifications are necessary to allow for low-energy pathways leading from the $(NO_2)_2$ radical-pair intermediate to both the final products *trans*-$ONONO_2$ and *sym*-N_2O_4 as depicted in Scheme 2.

Experimental Section

Chemicals: NO was made from the reaction of sulfuric acid, mercury and $NaNO_3$ (Merck). A 250 mL glass bulb equipped with a 10 mm Young valve was charged with $NaNO_3$ (680 mg, 8 mmol) and mercury (15 g, 75 mmol) and was then evacuated. An aqueous H_2SO_4 solution (20 wt %, ca. 10 g) was slowly introduced through the valve into the evacuated reaction vessel. The contents were shaken for 1 h at room temperature, and the gaseous reaction products were passed through three U-traps maintained at −100, −183 and −196 °C in a dynamic vacuum. Subsequently the trap at −196 °C contained 6 mmol of pure NO.

Oxygen (99.99 %, Messer-Griesheim), $^{18}O_2$ (99 % Campro) and neon (99.999 % Linde) were used without further purification. $N(^{16/18}O)_2$ isotopologues were produced in a pre-cleaned 500 mL Duran glass reactor kept in the dark at ambient temperatures. 99 % pure $^{18}O_2$ was mixed with $N^{16}O$ in a 1:2 ratio at a total pressure of 50 mbar. After about 10 min, an aliquot of the gaseous mixture was admitted into an infrared cell connected to the Duran vacuum line. The IR spectrum revealed that complete isotopic scrambling occurred, and that all three possible $N(^{16/18}O)_2$ isotopologues were formed.

Preparation of the matrices: Details of the matrix apparatus have been described elsewhere.[116]

A pure NO_2 sample (ca. 1 mmol) was transferred in vacuo into a thoroughly dried, small U-trap kept at −100 °C for about 1 h. This U-trap was mounted in front of the matrix support and allowed to reach a temperature of −115 °C in a cold bath. Gas streams (1–3 $mmol\,h^{-1}$) of neon were directed over the cold sample in the U-trap and through a cooled transfer line and spray-on nozzle (−78°) onto the matrix support cooled to 6.3 K.

In the experiments using Ne/NO and Ne/O_2 the corresponding gaseous mixtures were premixed in a 1 L stainless steel cylinder (Ne/NO 800:1–2) and a 500 mL Duran glass flask (Ne/O_2 400:2–10), respectively. The samples (2 mmol) were than transferred from these reservoirs through stainless steel capillaries to a cooled nozzle (≈85 K) where they were mixed in front of the matrix support at low pressures and co-deposited on the cold Rh mirror at 6.3 K at a rate of 2 $mmol\,h.^{-1}$

Instrumentation: Matrix IR spectra were recorded on a IFS 66v FT spectrometer (Bruker) equipped with a special transfer optic for measurements in the reflectance mode. A liquid-helium-cooled Si bolometer (Infrared Laboratories), together with a 6 μm Ge-coated Mylar beam splitter, were used in the region 650 to 80 cm^{-1}. In the 500 to 4000 cm^{-1} range, a MCT500 detector in combination with a KBr/Ge beam splitter was used. 100 scans were co-added for each spectrum using apodised resolutions of 0.25 and 0.75 cm^{-1}, respectively.

UV/Vis spectra were measured with a Perkin–Elmer Lambda 900 UV spectrometer in the range of 200 to 800 nm with a data-point separation of 1 nm and an integration time of 2 s. The radiation of the spectrometer was directed into a optical quartz fibre (150 cm long) through a quartz lens inside the cryostat and twice passed through the matrix deposited on the cold Rh mirror. A second quartz lens and fibre collected the reflected radiation and directed it into the spectrometer.

UV/Vis photolysis experiments were carried out using a ArF excimer laser (OPTEX, Lambda Physik) and a high-pressure mercury lamp (TQ 150, Heraeus) or a tungsten halogen lamp (250 W, Osram) in combination with a water-cooled quartz lens and different filters. In the UV region, a band-pass filter for the wavelength range between 260 and 400 nm (Schott, UG11, $d=3$ mm) was used. IR radiation was subjected to the deposit through a combination of KBr ($d=5$ mm) and silicon ($d=$ 1 mm) windows using a globar source centred in a parabolic mirror.

Quantum chemical calculations: Quantum-chemical calculations were carried out at the DFT[117] level by employing the B3LYP hybrid functional method[79] combined with the 6-311+G(2d) basis set[118,119] and the complete basis set CBS-QB3 methodology,[82] in which B3LYP DFT[79] is combined with the 6-311G(2d,d,p) basis set. These calculations were performed with the Gaussian 03W program package.[120] Computed stationary points were characterised by evaluating the corresponding harmonic

force field, and harmonic vibrational wavenumbers were computed by means of analytic second derivatives.

Molecular geometries and relative energies of various $ONONO_2$ isomers were also optimised using different DFT functionals (PBE,[90] B2PLYP[91] and B3LYP[79]) augmented with an empirical correction for long-range dispersion interactions ("PBE-D", "B2PLYP-D" and "B3LYP-D"),[88,89] and by ab initio spin-component-scaled second-order Møller–Plesset perturbation theory[85] (SCS-MP2).[86,87] These calculations were performed using the TURBOMOLE program package.[121] In the B2PLYP-D calculation, the TZVPP[122] basis set was used, whereas in the other calculations the larger def2-QZVP[123] basis set was employed throughout. The quadratic force field and harmonic frequencies of the $ONONO_2$ species were evaluated analytically in the B3LYP-D calculations, whereas the harmonic frequencies obtained at the SCS-MP2 level have been determined numerically.

Acknowledgements

We are grateful to Prof. S. Grimme, and particularly to Dr. C. Mück-Lichtenfeld for providing their results of SCS-MP2 and DFT-D calculations on various $ONONO_2$ isomers, and to a referee, who drew our attention to these theoretical methods. It is a pleasure to thank Dr. M. Jacox and Dr. W. Eisfeld for reading and criticizing an early draft of this article. This work was supported by the Deutsche Forschungsgemeinschaft and the Fonds der Chemischen Industrie. H.B. appreciates support from the Forschungszentrum Jülich GmbH, and X.Z. acknowledges a fellowship from the Alexander von Humboldt Foundation.

[1] H. Beckers, H. Willner, M. E. Jacox, *ChemPhysChem* **2009**, *10*, 706–710.
[2] B. J. Finlayson-Pitts, J. N. Pitts, Jr., *Science* **1997**, *276*, 1045–1051.
[3] M. J. Clarke, J. B. Gaul in *Structure and Bonding, Vol. 81*, Springer, Berlin, **1993**, pp. 148–181.
[4] M. Kirsch, H.-G. Korth, R. Sustmann, H. de Groot, *Biol. Chem.* **2002**, *383*, 389–399.
[5] T. Congedo, E. Lahoda, R. Matzie, K. Task in *Kent and Riegel's Handbook of Industrial Chemistry and Biotechnology, Vol. II*, 11th ed. (Ed.: J. A. Kent), Springer, New York, **2007**, pp. 996–1085.
[6] K. Miaskiewicz, K. Zbigniew, *J. Solution Chem.* **1990**, *19*, 465–471.
[7] D. A. Pinnick, S. F. Agnew, B. I. Swanson, *J. Phys. Chem.* **1992**, *96*, 7092–7096.
[8] A. J. Vosper, *J. Chem. Soc. A* **1970**, 2191–2193.
[9] B. Andrews, A. Anderson, *Chem. Phys.* **1981**, *55–63*, 1534–1537.
[10] S. F. Agnew, B. I. Swanson, L. H. Jones, R. L. Mills, D. Schiferl, *J. Phys. Chem.* **1983**, *87*, 5065–5068.
[11] A. Givan, A. Loewenschuss, *J. Chem. Phys.* **1990**, *93*, 866–867.
[12] T. G. Koch, A. B. Horn, M. A. Chester, M. R. S. McCoustra, J. R. Sodeau, *J. Phys. Chem.* **1995**, *99*, 8362–8367.
[13] E. J. Sluyts, B. J. Van der Veken, *J. Mol. Struct.* **1994**, *320*, 249–267.
[14] R. F. Holland, W. B. Maier II, *J. Chem. Phys.* **1983**, *78*, 2928–2941.
[15] L. Parts, J. T. Miller, Jr., *J. Chem. Phys.* **1965**, *43*, 136–139.
[16] A. K. Vorob'ev, A. A. Revsina, V. S. Gurman, *Russ. Chem. Bull.* **1996**, *105*, 809–813.
[17] F. Bolduan, H. J. Jodl, *Chem. Phys. Lett.* **1982**, *85*, 283–286.
[18] H. Bandow, H. Akimoto, S. Akiyama, T. Tezuka, *Chem. Phys. Lett.* **1984**, *111*, 496–500.
[19] F. Ding, X.-F. Wang, Q. Qin, *Fudan Xuebao Ziran Kexueban* **1999**, *38*, 89–92.
[20] R. V. St. Louis, B. Crawford, Jr., *J. Chem. Phys.* **1965**, *42*, 857–864.
[21] G. R. Smith, W. A. Guillory, *J. Mol. Spectrosc.* **1977**, *68*, 223–235.
[22] E. L. Varetti, G. C. Pimentel, *J. Chem. Phys.* **1971**, *55*, 3813–3821.
[23] A. Yabushita, Y. Inoue, T. Senga, M. Kawasaki, S. Sato, *J. Phys. Chem. A* **2004**, *108*, 438–446.
[24] J. Wang, B. E. Koel, *Surf. Sci.* **1999**, *436*, 15–28.
[25] A. J. Vosper, *J. Chem. Soc. A* **1970**, 625–627.
[26] W. N. Sisk, C. E. Miller, H. S. Johnston, *J. Phys. Chem.* **1993**, *97*, 9916–9923.
[27] C. Morrell, C. Breheny, V. Haverd, A. Cawley, G. Hancock, *J. Chem. Phys.* **2002**, *117*, 11121–11130.
[28] W. Li, X. Zhou, R. Lock, S. Patchkovskii, A. Stolow, C. Kapteyn, M. M. Murnane, *Science* **2008**, *322*, 1207–1211.
[29] E. D. Glendening, A. M. Halpern, *J. Chem. Phys.* **2007**, *127*, 164307, 1–11.
[30] F. R. Ornellas, S. M. Resende, F. Machado, B. C. O. Roberto-Neto, *J. Chem. Phys.* **2003**, *118*, 4060–4065.
[31] S. S. Wesolowski, J. T. Fermann, T. D. Crawford, H. F. Schaefer III, *J. Chem. Phys.* **1997**, *106*, 7178–7184.
[32] Y. Li, *J. Chem. Phys.* **2007**, *127*, 204502/1–6.
[33] H. Gershinowitz, H. Eyring, *J. Am. Chem. Soc.* **1935**, *57*, 985–991.
[34] S. Goldstein, G. Czapski, *J. Am. Chem. Soc.* **1995**, *117*, 12078–12084.
[35] G. R. Smith, W. A. Guillory, *Int. J. Chem. Kinet.* **1977**, *9*, 953–968.
[36] X.-F. Wang, Y.-Z. Xu, M. Yu, Q.-K. Zheng, *Acta Chim. Sin.* **1996**, *54*, 1186–1193.
[37] J. Olbregts, *Int. J. Chem. Kinet.* **1985**, *17*, 835–848.
[38] B. Galliker, R. Kissner, T. Nauser, W. H. Koppenol, *Chem. Eur. J.* **2009**, *15*, 6161–6168.
[39] M. L. McKee, *J. Am. Chem. Soc.* **1995**, *117*, 1629–1637.
[40] L. P. Olson, K. T. Kuwata, M. D. Bartberger, K. N. Houk, *J. Am. Chem. Soc.* **2002**, *124*, 9469–9475.
[41] O. B. Gadzhiev, S. K. Ignatov, A. G. Razuvaev, A. E. Masunov, *J. Phys. Chem. A* **2009**, *113*, 9092–9101.
[42] J. Laane, J. R. Ohlsen in *Progress in Inorganic Chemistry, Vol. 27* (Ed.: S. J. Lippard), Wiley, New York, **1980**, pp. 465–513.
[43] L. H. Jones, B. I. Swanson, S. F. Agnew, *J. Chem. Phys.* **1985**, *82*, 4389–4390.
[44] A. Givan, A. Loewenschuss, *Struct. Chem.* **1990**, *1*, 579–582.
[45] Y. Meng, R. B. Von Dreele, B. H. Toby, P. Chow, M. Y. Hu, G. Shen, H.-k. Mao, *Phys. Rev. B* **2006**, *74*, 214107,1–5.
[46] Y. Song, R. J. Hemley, Z. Liu, M. Somayazulu, H.-k. Mao, D. R. Herschbach, *J. Chem. Phys.* **2003**, *119*, 2232–2240.
[47] F. Bolduan, H. J. Jodl, A. Loewenschuss, *J. Chem. Phys.* **1984**, *80*, 1739–1743.
[48] J. A. Bacon, C. F. Giese, W. R. Gentry, *J. Chem. Phys.* **1998**, *108*, 3127–3133.
[49] J. B. Nee, C. Y. Juan, J. Y. Hsu, J. C. Yang, W. J. Chen, *Chem. Phys.* **2004**, *300*, 85–92.
[50] E. P. F. Lee, T. G. Wright, *Chem. Phys. Lett.* **2001**, *347*, 429–435.
[51] W. Eisfeld, K. Morokuma, *J. Chem. Phys.* **2003**, *119*, 4682–4688.
[52] G. Chalasinski, M. M. Szczesniak, *Chem. Rev.* **2000**, *100*, 4227–4252.
[53] M. E. Jacox, W. E. Thompson, *J. Chem. Phys.* **2008**, *129*, 204306/1–15.
[54] F. Cacace, G. de Petris, M. Rosi, A. Troiani, *Chem. Eur. J.* **2002**, *8*, 5684–5693.
[55] E. Frears, N. Nazhat, D. Blake, M. Symons, *Free Radical Res.* **1997**, *27*, 31–35.
[56] C. Amatore, S. Arbault, D. Bruce, P. de Oliveira, M. Erard, M. Vuillaume, *Chem. Eur. J.* **2001**, *7*, 4171–4179.
[57] Experimental enthalpies of formation are taken from the NIST Chemistry Webbook, NIST Standard Reference Database Number 69; March 2003 Release, http://webbook.nist.gov/chemistry. Enthalpies of formation of the proposed intermediates $ON{\cdot}O_2$ and *s-cis,cis*-ONOONO are not reported. The free Gibbs energy of formation of the $ON{\cdot}O_2$ complex was recently estimated to be $\Delta_f G^\ominus \approx (+102 \pm 10)\,kJ\,mol^{-1}$ from the electrode potential $E^\ominus(ON{\cdot}O_2/ONOO^-)$ measured in aqueous solution (ref. [38]). Therein we assumed $\Delta_f H^\ominus \approx 88\,kJ\,mol^{-1}$ for this complex, estimated from the enthalpy of formation of NO ($\Delta_f H^\ominus = 90.3\,kJ\,mol^{-1}$) and the calculated bond energy of this complex of about 1–2 $kJ\,mol^{-1}$ (ref. [39]). For the peroxide *s-cis,cis*-ONOONO we have chosen the computational predicted value of $\Delta_f H^\ominus \approx 140\,kJ\,mol^{-1}$ (ref. [39]), however, more recent calculations (ref. [41]) predict $\Delta_f H^\ominus \approx 170\,kJ\,mol^{-1}$ for this peroxide.

[58] ONOONO was assumed to be the carrier of a diamagnetic red intermediate formed when NO was suspended into a solution of O_2 in 2-methylbutane at 130 K (ref. [38]). As mentioned therein, a very similar visible spectrum was reported for a species formed from nitric oxide and various Lewis acids at 77 K, which has been attributed to the asymmetric $(NO)_2$ dimer, O-N-O-N (see ref. [46] in ref. [38]). In a former study (ref. [15]) a red solid was obtained in a similar experiment using an ethane/propane solution at 79 K. The red solid was attributed to nitrosonium nitrate based on the infrared spectra of the solution and the solid. Pertinent to these observations is also a more recent work (ref. [16]) on the photochemistry of *sym*-N_2O_4 in a matrix of glassy methylcyclohexane in the temperature range 77–100 K, in which the formation of $NO^+NO_3^-$ was also proposed.
[59] A. S. Pimentel, F. C. A. Lima, A. B. F. da Silva, *J. Phys. Chem. A* **2007**, *111*, 2913–2920.
[60] C. L. Lv, Y. D. Liu, R. Zhong, *J. Phys. Chem. A* **2008**, *112*, 7098–7105.
[61] I. I. Zakharov, A. I. Kolbasin, O. I. Zakharova, I. V. Kravchenko, V. I. Dyshlovoi, *Theor. Exp. Chem.* **2008**, *44*, 26–31.
[62] H. D. Sharma, R. E. Jervis, K. Y. Wong, *J. Phys. Chem.* **1970**, *74*, 923–933.
[63] B. J. Finlayson-Pitts, L. M. Wingen, A. L. Sumner, D. Syomin, K. A. Ramazan, *Phys. Chem. Chem. Phys.* **2003**, *5*, 223–242.
[64] A. S. Pimentel, F. C. A. Lima, A. B. F. da Silva, *Chem. Phys. Lett.* **2007**, *436*, 47–50.
[65] F. Legay, N. Legay-Sommaire, *Chem. Phys. Lett.* **1993**, *211*, 516–522.
[66] F. Mélen, F. Pokorni, M. Herman, *Chem. Phys. Lett.* **1992**, *194*, 181–186.
[67] D. W. Green, S. D. Gabelnick, G. T. Reedy, *J. Chem. Phys.* **1976**, *64*, 1697–1705.
[68] Note that the choice of axis labels for the particular molecule of consideration is somewhat arbitrary; b_{1u} is taken for the out-of-plane vibration, and b_{2u} and b_{3u} denote in-plane representations perpendicular and parallel to the N–N bond axis, respectively.
[69] J. Koput, J. W. G. Seibert, B. P. Winnewisser, *Chem. Phys. Lett.* **1993**, *204*, 183–189.
[70] R. Kometer, F. Legay, N. Legay-Sommaire, N. Schwentner, *J. Chem. Phys.* **1994**, *100*, 8737–8745.
[71] F. Legay, N. Legay-Sommaire, *J. Chem. Phys.* **1995**, *102*, 7798–7806.
[72] L. Krim, N. Lacome, *J. Phys. Chem. A* **1998**, *102*, 2289–2296.
[73] L. Krim, *J. Mol. Struct.* **1998**, *471*, 267–273.
[74] J. R. Hetzler, M. P. Casassa, D. S. King, *J. Phys. Chem.* **1991**, *95*, 8086–8095.
[75] A. B. Potter, V. Drbinski, A. V. Demyanenko, H. Reisler, *J. Chem. Phys.* **2003**, *119*, 7197–7205.
[76] Y. Matsumoto, Y. Ohshima, M. Takami, *J. Chem. Phys.* **1990**, *92*, 937–942.
[77] D. L. Cocke, J. A. G. Gomes, J. L. Gossage, K. Li, C.-J. Lin, S. Tandel, *Appl. Spectrosc.* **2004**, *58*, 528–534.
[78] C.-I. Lee, Y.-P. Lee, X. Wang, Q.-Z. Qin, *J. Chem. Phys.* **1998**, *109*, 10446–10455.
[79] A. D. Becke, *J. Chem. Phys.* **1993**, *98*, 5648–5652.
[80] A. Kovács, K. B. Borisenko, G. Pongor, *Chem. Phys. Lett.* **1997**, *280*, 451–458.
[81] X. Wang, Q.-Z. Qin, K. Fan, *J. Mol. Struct.* **1998**, *440–473*, 55–62.
[82] J. A. Montgomery, Jr., M. J. Frisch, J. W. Ochterski, G. A. Petersson, *J. Chem. Phys.* **2000**, *112*, 6532–6542.
[83] L. Noodleman, E. R. Davidson, *Chem. Phys.* **1986**, *109*, 131–143.
[84] D. A. Singleton, C. Hang, M. J. Szymanski, M. P. Meyer, A. G. Leach, K. T. Kuwata, J. S. Chen, A. Greer, C. S. Foote, K. N. Houk, *J. Am. Chem. Soc.* **2003**, *125*, 1319–1328.
[85] C. Møller, M. S. Plesset, *Phys. Rev.* **1934**, *46*, 618–622.
[86] S. Grimme, *J. Chem. Phys.* **2003**, *118*, 9095–9102.
[87] M. Gerenkamp, S. Grimme, *Chem. Phys. Lett.* **2004**, *392*, 229–235.
[88] S. Grimme, *J. Comput. Chem.* **2004**, *25*, 1463–1473.
[89] S. Grimme, *J. Comput. Chem.* **2006**, *27*, 1787–1799.
[90] J. P. Perdew, K. Burke, M. Ernzerhof, *Phys. Rev. Lett.* **1996**, *77*, 3865–3868.
[91] S. Grimme, *J. Chem. Phys.* **2005**, *122–123*, 034108/1–16.
[92] H. Oberhammer, *J. Mol. Struct.* **2002**, *605*, 177–185.
[93] I. Love, *J. Phys. Chem. A* **2006**, *110*, 10507–10512.
[94] P. Felder, T.-K. Ha, A. M. Dwivedi, H. H. Günthard, *Spectrochim. Acta* **1981**, *37A*, 337–345.
[95] J. M. Coanga, L. Schriver-Mazzuoli, A. Schriver, P. R. Dahoo, *Chem. Phys.* **2002**, *276*, 309–320.
[96] A. J. Kirby, *The Anomeric Effect and Related Stereoelectronic Effects at Oxygen*, Springer, Berlin, **1983**.
[97] T. Yamamoto, D. Kaneno, S. Tomoda, *J. Org. Chem.* **2008**, *73*, 5429–5435.
[98] B. F. Parsons, S. L. Curry, J. A. Mueller, P. C. Ray, L. J. Butler, *J. Chem. Phys.* **1999**, *111*, 8486–8495.
[99] S. Sato, T. Senga, M. Kawasaki, *J. Phys. Chem. B* **1999**, *103*, 5063–5069.
[100] R. Jost, J. Nygard, A. Pasinski, A. Delon, *J. Chem. Phys.* **1996**, *105*, 1287–1290.
[101] M. F. Merienne, A. Jenouvrier, B. Coquart, J. P. Lux, *J. Atmos. Chem.* **1997**, *27*, 219–232.
[102] A. J. Downs, G. P. Gaskill, S. B. Saville, *Inorg. Chem.* **1982**, *21*, 3385–3393.
[103] M. Chen, X. Wang, L. Zhang, Q. Qin, Q. Zheng, *Chem. Phys.* **2000**, *255-262*, 95–102.
[104] A. Stirling, I. Pápai, J. Mink, D. R. Salahub, *J. Chem. Phys.* **1994**, *100*, 2910–2923.
[105] L. Bencivenni, N. Sanna, L. Schriver-Mazzuoli, A. Schriver, *J. Chem. Phys.* **1996**, *104*, 7836–7846.
[106] N. Dozova, L. Krim, M. E. Alikhani, N. Lacome, *J. Phys. Chem. A* **2006**, *110*, 11617–11626.
[107] A. de Saxce, N. Sanna, A. Schriver, L. Schriver-Mazzuoli, *Chem. Phys.* **1994**, *185*, 365–383.
[108] K. A. Ramazan, D. Syomin, B. J. Finlayson-Pitts, *Phys. Chem. Chem. Phys.* **2004**, *6*, 3836–3843.
[109] Y. Miller, B. J. Finlayson-Pitts, R. B. Gerber, *J. Am. Chem. Soc.* **2009**, 131, 12180–12185.
[110] W.-J. Lo, Y.-P. Lee, *J. Chem. Phys.* **1994**, *101*, 5494–5499.
[111] G. Merényi, J. Lind, *Chem. Res. Toxicol.* **1998**, *11*, 243–246.
[112] K. W. Scholtens, B. M. Messer, C. D. Cappa, M. J. Elrod, *J. Phys. Chem. A* **1999**, *103*, 4378–4384.
[113] D. E. Tevault, R. R. Smardzewski, *J. Phys. Chem.* **1978**, *82*, 375–378.
[114] D. W. T. Griffith, G. S. Tyndall, J. P. Burrows, G. K. Moortgat, *Chem. Phys. Lett.* **1984**, *107*, 341–346.
[115] Y. Zhao, K. N. Houk, L. P. Olson, *J. Phys. Chem. A* **2004**, *108*, 5864–5871.
[116] H. G. Schnöckel, H. Willner in *Infrared and Raman Spectroscopy, Methods and Applications* (Ed.: B. Schrader), VCH, Weinheim, **1994**.
[117] R. G. Parr, W. Yang in *Density-Functional Theory of Atoms and Molecules*, Academic Press, London, **1994**.
[118] A. D. McLean, G. S. Chandler, *J. Chem. Phys.* **1980**, *72*, 5639–5648.
[119] R. Krishnan, J. S. Binkley, R. Seeger, J. A. Pople, *J. Chem. Phys.* **1980**, *72*, 650–654.
[120] Gaussian 03, Revision D.01, M. J. Frisch, G. W. Trucks, H. B. Schlegel, G. E. Scuseria, M. A. Robb, J. R. Cheeseman, J. A. Montgomery, Jr., T. Vreven, K. N. Kudin, J. C. Burant, J. M. Millam, S. S. Iyengar, J. Tomasi, V. Barone, B. Mennucci, M. Cossi, G. Scalmani, N. Rega, G. A. Petersson, H. Nakatsuji, M. Hada, M. Ehara, K. Toyota, R. Fukuda, J. Hasegawa, M. Ishida, T. Nakajima, Y. Honda, O. Kitao, H. Nakai, M. Klene, X. Li, J. E. Knox, H. P. Hratchian, J. B. Cross, V. Bakken, C. Adamo, J. Jaramillo, R. Gomperts, R. E. Stratmann, O. Yazyev, A. J. Austin, R. Cammi, C. Pomelli, J. W. Ochterski, P. Y. Ayala, K. Morokuma, G. A. Voth, P. Salvador, J. J. Dannenberg, V. G. Zakrzewski, S. Dapprich, A. D. Daniels, M. C. Strain, O. Farkas, D. K. Malick, A. D. Rabuck, K. Raghavachari, J. B. Foresman, J. V. Ortiz, Q. Cui, A. G. Baboul, S. Clifford, J. Cioslowski, B. B. Stefanov, G. Liu, A. Liashenko, P. Pis-

korz, I. Komaromi, R. L. Martin, D. J. Fox, T. Keith, M. A. Al-Laham, C. Y. Peng, A. Nanayakkara, M. Challacombe, P. M. W. Gill, B. Johnson, W. Chen, M. W. Wong, C. Gonzalez, J. A. Pople, Gaussian Inc., Wallingford CT, **2004**.

[121] R. Ahlrichs, M. Bär, H.-P. Baron, R. Bauernschmitt, S. Böcker, M. Ehrig, K. Eichkorn, S. Elliot, F. Furche, F. Haase, M. Häser, H. Horn, C. Huber, U. Huniar, M. Kattanek, C. Kölmel, M. Kollwitz, K. May, C. Ochsenfeld, H. Öhm, A. Schäfer, U. Schneider, O. Treutler, M. von Armin, F. Weigend, P. Weis, H. Weiss, Universität Karlsruhe, **2003**.

[122] A. Schäfer, C. Huber, R. Ahlrichs, *J. Chem. Phys.* **1994**, *100*, 5829–5835.

[123] F. Weigend, R. Ahlrichs, *Phys. Chem. Chem. Phys.* **2005**, *7*, 3297–3305.

Received: August 31, 2009
Published online: December 18, 2009

